



HAL
open science

Study of performance criteria of serial configuration of two chemostats

Manel Dali Youcef, Alain Rapaport, Tewfik Sari

► **To cite this version:**

Manel Dali Youcef, Alain Rapaport, Tewfik Sari. Study of performance criteria of serial configuration of two chemostats. *Mathematical Biosciences and Engineering*, 2020, 17 (6), pp.6278-6309. 10.3934/mbe.2020332 . hal-02935942

HAL Id: hal-02935942

<https://hal.inrae.fr/hal-02935942v1>

Submitted on 10 Sep 2020

HAL is a multi-disciplinary open access archive for the deposit and dissemination of scientific research documents, whether they are published or not. The documents may come from teaching and research institutions in France or abroad, or from public or private research centers.

L'archive ouverte pluridisciplinaire **HAL**, est destinée au dépôt et à la diffusion de documents scientifiques de niveau recherche, publiés ou non, émanant des établissements d'enseignement et de recherche français ou étrangers, des laboratoires publics ou privés.

STUDY OF PERFORMANCE CRITERIA OF SERIAL CONFIGURATION OF TWO CHEMOSTATS

MANEL DALI YOUCEF, ALAIN RAPAPORT AND TEWFIK SARI

ABSTRACT. This paper deals with thorough analysis of serial configurations of two chemostats. We establish an in-depth mathematical study of all possible steady states, and we compare the performances of the two serial interconnected chemostats with the performances of a single one. The comparison is evaluated under three different criteria. We analyze, at steady state, the minimization of the output substrate concentration, the productivity of the biomass and the biogas flow rate. We determine specific conditions, which depend on the biological parameters, the operating parameters of the model and the distribution of the total volume. These necessary and sufficient conditions provide the most efficient serial configuration of two chemostats versus one. Complementarily, this mainly helps to discern when it is not advisable to use the serial configuration instead of a simple chemostat, depending on: the considered criterion, the operating parameters fixed by the operator and the distribution of the volumes into the two tanks.

1. INTRODUCTION

The chemostat device was invented concomitantly by Monod [1] and Novick & Szilard [2] in 1950. Widely used as a biochemical laboratory-pilot, it consists essentially in a continuously-fed bioreactor characterized by the equality of the input and the output flow rates. It is designed as a vessel in which different microorganisms grow, also called continuous culture of microorganisms. Its importance for the continuous culture of microorganisms has been reported in several books and publications, among them [3, 4, 5, 6, 7]. In other words, the classical model of the chemostat consists of a perfect mixed media at a constant temperature, a constant pH, a filtered feed and a unique flow rate. Although this model is used for industrial applications with continuously-fed bioreactors such as wastewater treatment, see for instance [8], in physical reality, industrial applications which use large bioreactors hardly satisfy the assumption of the perfect mixed media. Several mathematical representations of the spatial heterogeneity have been studied in the literature with partial differential equations, see for instance [9, 10]. However, discrete spatial representations, such as the gradostat model [6, 11], are also a way to represent spatial heterogeneity [12, 13, 14]. Serial configurations, as a simple gradostat, have received a great interest in the literature in view of optimizing bioprocesses. Indeed, it has been shown that having two tanks (or more) in series (each of them being assumed to be perfectly mixed) can produce the same substrate conversion than a single vessel, but with a significant lower total volume, and thus a lower residence time. Serial configurations have been also studied in view of ecological insight, see for instance [15, 16]. In this paper, we propose to revisit the serial configuration of two chemostats in series with a constant total volume V , as shown in Figure 1. We focus on the analysis of the performance at steady-state for different criteria with the aim of drawing comparisons with the single chemostat. Notice that these different criteria of comparison are known in the literature, see for instance [3]. However, to our knowledge, a complete and deep analysis of all possible configurations for a general class

of growth functions and the various criteria is missing in the literature, which is the aim of the present work.

It is well known [4, 6] that, for the simple chemostat, the output concentration at steady state S^{out} is independent of the input concentration S^{in} , provided that there is no washout, see also (2.5). This property is no longer satisfied when there is a spatial structure, see for instance [15] and the references therein. Since S^{out} measures the performances of the chemostat to convert the substrate S , our purpose is to distinguish which configuration guarantees the minimal output substrate concentration at steady state. Actually, reducing the output substrate concentration is one of the biological objectives in waste-water treatments and this minimizing problem is well known in the literature. The novelty of our work is that S^{out} is considered as a function which depends on the three operating parameters: the input substrate concentration, the dilution rate and the volume of each chemostat. In fact, what has already been treated, see for instance [17, 18, 19], corresponds to the case where the input substrate concentration S^{in} is fixed and the total volume V can be chosen. Thus, we give conditions which involve the input substrate concentration S^{in} and ensure the optimal way to slice the two serial reactors volume. These conditions can ensure a lower output substrate concentration.

Our study is somehow a generalization of the main results presented in [16]. The conditions that we found are necessary and sufficient to reduce the output substrate concentration in contrast of the result in [16] where the given conditions are only sufficient. In addition, the originality of this article consists in comparing both configurations according to two other performance indexes which are the productivity of the biomass and the biogas flow rate. The biogas flow rate represents the quantity of natural gas per unit of time produced by the decomposition of organic matter in absence of oxygen and the productivity of the biomass represents the amount of biomass per unit of time produced by the decomposition of organic matter. The productivity of the biomass of several configurations including the serial device of two interconnected chemostats has been graphically and numerically analyzed in [12, 20]. However, these two criteria have not yet been deeply mathematically analyzed. The global analysis shows that the different performance criteria involve the same performance threshold. This threshold is explicitly defined by a function which depends on the dilution rate D . It defines the set of the values of S^{in} and D that allow or not a better performance of the serial configuration with two chemostats. Several numerical applications are given to illustrate all the results of the study.

This paper is organized as follows. Section 2 presents the model. Subsequently, the main part of the paper constituting Section 3 is dedicated to the study of the equilibria and the performance analysis of the configuration. Indeed, the output substrate concentration, the productivity of the biomass and the biogas flow rate are respectively treated in Sections 3.1, 3.2 and 3.3. Next, the operating diagram of the model is depicted in Section 4. Afterwards, several numerical simulations illustrating the results of our analysis and using some specific growth functions are represented in Section 5. Finally, Section 6 contains a global conclusion. Most of the proofs corresponding of the theorems and propositions stated along the paper are proved in Appendixes A, B, C and D. Firstly, Appendix A contains the proof related to the existence and the stability of steady states. Secondly, Appendixes B and C contain respectively the proofs related to the output substrate concentration, the productivity of the biomass and the biogas flow rate. Finally, Appendix D contains proofs related to some of technical results of the paper.

2. MATHEMATICAL MODEL

If S and X denote respectively the substrate and the biomass concentration in a single chemostat of volume V , the input flow rate Q and the input concentration of substrate S^{in} , their time evolution are modeled by the following system of ordinary differential equations:

$$(2.1) \quad \begin{aligned} \dot{S} &= D(S^{in} - S) - f(S)X/Y \\ \dot{X} &= -DX + f(S)X \end{aligned}$$

where Y is the yield conversion of substrate into biomass, $f(\cdot)$ the specific growth rate of the microorganisms that is assumed null at $S = 0$ and to be increasing for $S > 0$, and $D = Q/V$ is the dilution rate. Without loss of generality, one can assume $Y = 1$ in equations (2.1) by using the change of variable $x = X/Y$. System (2.1) becomes

$$(2.2) \quad \begin{aligned} \dot{S} &= D(S^{in} - S) - f(S)x \\ \dot{x} &= -Dx + f(S)x. \end{aligned}$$

The detailed mathematical analysis of the model (2.2) may be found in [4, 6]. Let us recall classical results about the asymptotic behavior of (2.2). We define

$$(2.3) \quad m := \sup_{S>0} f(S), \quad (m \text{ may be } +\infty).$$

As f is increasing then the *break-even concentration* is defined by

$$(2.4) \quad \lambda(D) := f^{-1}(D) \quad \text{when} \quad 0 \leq D < m.$$

When $S^{in} > \lambda(D)$ (or, equivalently, $f(S^{in}) > D$), any solution of (2.2) with $S(0) \geq 0$ and $x(0) > 0$ converges toward the positive steady state $E_1 = (\lambda(D), S^{in} - \lambda(D))$. On the contrary, when $D \geq m$ or $S^{in} \leq \lambda(D)$ (or, equivalently, $f(S^{in}) \leq D$), any solution of (2.2) with $S(0) \geq 0$ and $x(0) \geq 0$ converges toward the wash-out steady state $E_0 = (S^{in}, 0)$. Thus, the output concentration at steady state $S^{out}(S^{in}, D)$ is given by

$$(2.5) \quad S^{out}(S^{in}, D) = \begin{cases} S^{in} & \text{if } D \geq f(S^{in}) \\ \lambda(D) & \text{if } D < f(S^{in}). \end{cases}$$

We consider now the serial interconnected chemostats, where the volume V is divided into two volumes, rV and $(1-r)V$ with $r \in (0, 1)$, as shown in Figure 1, with Q the flow rate and S^{in} the input substrate concentration in the first chemostat. The mathematical model is given by the following equations:

$$(2.6) \quad \begin{aligned} \dot{S}_1 &= \frac{D}{r}(S^{in} - S_1) - f(S_1)x_1 \\ \dot{x}_1 &= -\frac{D}{r}x_1 + f(S_1)x_1 \\ \dot{S}_2 &= \frac{D}{1-r}(S_1 - S_2) - f(S_2)x_2 \\ \dot{x}_2 &= \frac{D}{1-r}(x_1 - x_2) + f(S_2)x_2 \end{aligned}$$

The dilution rates of the first and second chemostats are D/r and $D/(1-r)$, respectively, where D is the dilution rate, defined by $D := Q/V$, of the single chemostat of volume V and flow rate Q . For the limiting cases $r = 0$ and $r = 1$, these equations are not valid. Indeed, the limiting cases correspond to the single chemostat model defined by (2.2).

In [16], the mathematical analysis of (2.6) was performed for a linear growth function $f(S) = aS$ ($a > 0$) and numerical simulations were given for a Monod growth function $f(S) = mS/(K + S)$. The results of [16] were extended to Monod growth function and for increasing and concave growth function in [21].

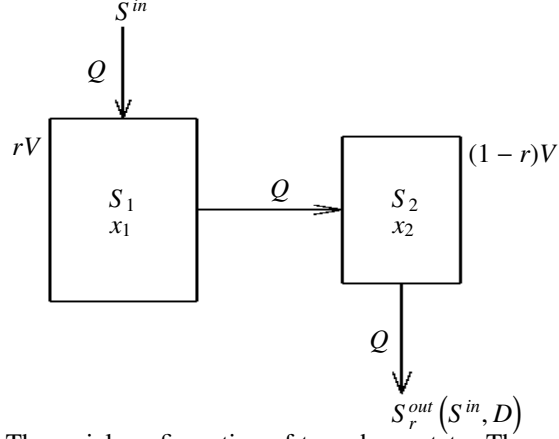


FIGURE 1. The serial configuration of two chemostats. The output substrate concentration at steady state S_r^{out} measures the performance of the system to convert the substrate S^{in} .

Remark 1. *The main result in [16, 21], see also [15], predicts that there exists a threshold S_1^{in} such that for $S^{in} \leq S_1^{in}$, the output $S_r^{out}(S^{in}, D)$, which is the output density of the substrate at steady state, satisfies $S_r^{out}(S^{in}, D) > \lambda(D)$, for all $r \in (0, 1)$ and, if $S^{in} > S_1^{in}$, there exists a threshold $r_1 \in (0, 1)$, such that $S_r^{out}(S^{in}, D) < \lambda(D)$ if and only if $r_1 < r < 1$.*

As it was noticed in (2.5), for a single chemostat, one has $S^{out}(S^{in}, D) = \lambda(D)$. Therefore, if $S^{in} \leq S_1^{in}$, the serial configuration is always less efficient than the single chemostat of the same total volume V . In contrast, for $S^{in} > S_1^{in}$ and r large enough (i.e. $r > r_1$), the serial configuration is more efficient than the single chemostat.

In this paper, we extend this result to general increasing growth functions where the concavity of f is not required and we provide explicit formulas for the thresholds $S_1^{in}(D)$ and $r_1(S^{in}, D)$. Hence, we consider a growth function satisfying only the following qualitative property:

Assumption 1. *The function f is C^1 , with $f(0) = 0$ and $f'(S) > 0$ for all $S > 0$.*

The following result is classical in the mathematical theory of the chemostat and is left to the reader.

Lemma 1. *The solutions $(S_1(t), x_1(t), S_2(t), x_2(t))$ of (2.6) with nonnegative initial conditions, exist for all $t \geq 0$, are nonnegative, bounded and $\lim_{t \rightarrow +\infty} (S_i(t) + x_i(t)) = S^{in}$ for $i = 1, 2$.*

The existence and stability of steady states of (2.6) are given by the following result. We use the abbreviation LES for locally exponentially stable and GAS for globally asymptotically stable in the positive orthant.

Theorem 1. *Assume that Assumption 1 is satisfied. The steady states of (2.6) are:*

- *The washout steady state $E_0 = (S^{in}, 0, S^{in}, 0)$ which always exists. It is GAS if and only if*

$$(2.7) \quad D \geq \max\{r, 1-r\}f(S^{in}).$$

It is LES if and only if: $D > \max\{r, 1-r\}f(S^{in})$.

- The steady state $E_1 = (S^{in}, 0, \bar{S}_2, S^{in} - \bar{S}_2)$ of washout in the first chemostat but not in the second one, where \bar{S}_2 is given by $\bar{S}_2 = \lambda(D/(1-r))$. This steady state exists if and only if $D < (1-r)f(S^{in})$. It is GAS if and only if

$$(2.8) \quad rf(S^{in}) \leq D < (1-r)f(S^{in}).$$

It is LES if and only if: $rf(S^{in}) < D < (1-r)f(S^{in})$.

- The steady state $E_2 = (S_1^*, S^{in} - S_1^*, S_2^*, S^{in} - S_2^*)$ of persistence of the species in both chemostats, where S_1^* is given by $S_1^* = \lambda(D/r)$ and $S_2^* = S_2^*(S^{in}, D, r)$ is the unique solution of the equation

$$(2.9) \quad h(S_2) = f(S_2) \quad \text{with} \quad h(S_2) := \frac{D(S_1^* - S_2)}{(1-r)(S^{in} - S_2)}.$$

This steady state exists if and only if $D < rf(S^{in})$. It is GAS and LES whenever it exists.

Proof. The proof is given in Appendix A. \square

Remark 2. Transcritical bifurcations occur in the limit cases $D = rf(S^{in})$ and $D = (1-r)f(S^{in})$.

- (1) For $0 < r < 1/2$, we have a transcritical bifurcation of E_0 and E_1 when $D = (1-r)f(S^{in})$ and a transcritical bifurcation of E_1 and E_2 when $D = rf(S^{in})$.
- (2) For $1/2 < r < 1$, we have a transcritical bifurcation of E_0 and E_2 when $D = rf(S^{in})$ and a transcritical bifurcation of E_0 and E_1 when $D = (1-r)f(S^{in})$.
- (3) For $r = 1/2$ and $D = f(S^{in})/2$, we have transcritical bifurcations of E_0 and E_1 , and E_0 and E_2 , simultaneously.

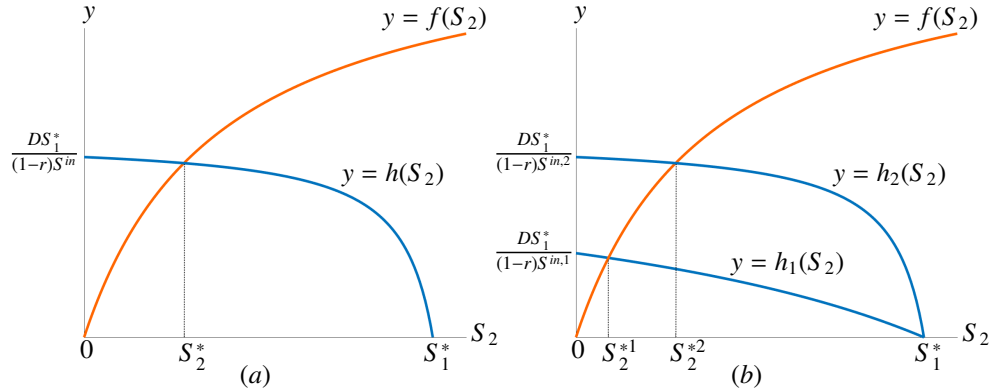


FIGURE 2. (a): Graphical illustration of equation (2.9). (b): The result of Proposition 1 with $S_2^{*i} = S_2^*(S^{in,i}, D, r)$, $i = 1, 2$.

Figure 2 (a) shows the functions f and h , and the solution $S_2^* = S_2^*(S^{in}, D, r)$ of the equation (2.9), which is unique since f is strictly increasing and the graph of h is a hyperbola. If $S^{in,1} > S^{in,2}$, then $h_i(S_2) = \frac{D(S_1^* - S_2)}{(1-r)(S^{in,i} - S_2)}$, $i = 1, 2$, satisfies $h_2(S_2) > h_1(S_2)$, for all $S_2 \in (0, S_1^*)$, as shown in Figure 2 (b). Therefore, we have the following result:

Proposition 1. Let $S^{in,1}$ and $S^{in,2}$ be two different input substrate concentrations. If $S^{in,1} > S^{in,2} > 0$ then for all $r \in (D/f(S^{in,2}), 1)$ and $D > 0$, one has $S_2^*(S^{in,1}, D, r) < S_2^*(S^{in,2}, D, r)$.

Proof. The proof is given in Appendix B.1. \square

3. THE THREE PERFORMANCE CRITERIA

In this section we give the expressions of the output substrate concentration at steady state, the productivity of the biomass and the biogas flow rate, for the serial configuration of two chemostats.

3.1. Output substrate concentration. Let us consider the dependency of the output substrate concentration with respect to the dilution rate D and the input concentration S^{in} . As stated in Theorem 1, for $0 < r < 1$, the output substrate concentration at steady state is given by the formulas:

$$(3.1) \quad S_r^{out}(S^{in}, D) = \begin{cases} S^{in} & \text{if } \max\{r, 1-r\}f(S^{in}) \leq D \\ \lambda(D/(1-r)) & \text{if } rf(S^{in}) \leq D \leq (1-r)f(S^{in}) \\ S_2^*(S^{in}, D, r) & \text{if } D < rf(S^{in}). \end{cases}$$

Although $S_r^{out}(S^{in}, D)$ is defined by (3.1) only for $0 < r < 1$, we extend it, by continuity, for $r = 0$ and $r = 1$ by

$$(3.2) \quad S_0^{out}(S^{in}, D) = S_1^{out}(S^{in}, D) = S^{out}(S^{in}, D).$$

The continuity follows from the facts that $\lim_{r \rightarrow 1} S_2^*(S^{in}, D, r) = \lambda(D)$ and the second case, where $S_r^{out}(S^{in}, D) = \lambda(D/(1-r))$, is possible only if $0 \leq r \leq 1/2$.

We have to compare $S_r^{out}(S^{in}, D)$, given by (3.1) and (3.2), with $S^{out}(S^{in}, D)$, given by (2.5). Let $r \in (0, 1)$ be fixed. Let $g_r : [0, rm) \rightarrow \mathbb{R}$, where m is given by (2.3), be defined by

$$(3.3) \quad g_r(D) := \lambda(D) + \frac{\lambda(D/r) - \lambda(D)}{1-r}.$$

The following result asserts that the serial configuration of two chemostats of volumes rV and $(1-r)V$ respectively, shown in Figure 1, is more efficient than the simple chemostat of volume V , if and only if $S^{in} > g_r(D)$.

Theorem 2. *For any $r \in (0, 1)$, one has $S_r^{out}(S^{in}, D) < S^{out}(S^{in}, D)$ if and only if $S^{in} > g_r(D)$.*

Proof. The proof is given in Appendix B.2 \square

We need the following assumption, which is satisfied by any concave growth function, but also by Hill function, which is not concave, as it is shown in Section 5.

Assumption 2. *For every $D \in [0, m)$, the function $r \in (D/m, 1) \mapsto g_r(D) \in \mathbb{R}$ is strictly decreasing.*

Let $g : [0, m) \mapsto \mathbb{R}$ be defined by

$$(3.4) \quad g(D) := \lambda(D) + \frac{D}{f'(\lambda(D))}.$$

We have the following result:

Lemma 2. *Assume that Assumptions 1 and 2 are satisfied. For all (S^{in}, D) verifying the condition $S^{in} > g(D)$, there exists a unique $r_1 = r_1(S^{in}, D) \in (0, 1)$ such that $S^{in} = g_{r_1}(D)$. One has $r > r_1(S^{in}, D)$ if and only if $S^{in} > g_r(D)$.*

Proof. The proof is given in Appendix B.3. \square

We can state now our main result which compares $S_r^{out}(S^{in}, D)$ and $S^{out}(S^{in}, D)$.

Theorem 3. *Assume that Assumptions 1 and 2 are satisfied.*

- If $S^{in} \leq g(D)$ then for any $r \in (0, 1)$, $S_r^{out}(S^{in}, D) > S^{out}(S^{in}, D)$.
- If $S^{in} > g(D)$ then $S_r^{out}(S^{in}, D) < S^{out}(S^{in}, D)$ if and only if $r_1(S^{in}, D) < r < 1$ with $r_1(S^{in}, D)$ defined in Lemma 2.

The equality is fulfilled for $r = 0$, $r = r_1$ and $r = 1$.

Proof. The proof is given in Appendix B.4. □

Lemma 2 and Theorem 3 give analytical expression for the thresholds S_1^{in} and r_1 mentioned in Remark 1. Indeed, we have $S_1^{in} = g(D)$ and r_1 depends on D and S^{in} , and is given implicitly by equation $S^{in} = g_{r_1}(D)$. In Section 5, we give explicit formulas for $r_1(S^{in}, D)$ in the cases of linear growth functions, see (5.1), or Monod growth functions, see (5.2). To have a better understanding of the role of the parameter r , we also analyze the function $r \mapsto S_r^{out}(S^{in}, D)$ when S^{in} and D are fixed. According to the conditions on S^{in} and D , related to the global stability of the equilibria, several cases must be distinguished. The following result encompasses the whole possible cases.

Proposition 2. *Let $D > 0$ and $S^{in} > 0$. We denote by r_0 the ratio $r_0 = D/f(S^{in})$.*

- 1) *If $S^{in} \leq \lambda(D)$ then for any $r \in [0, 1]$, one has $S_r^{out}(S^{in}, D) = S^{out}(S^{in}, D) = S^{in}$.*
- 2) *If $\lambda(D) < S^{in} < \lambda(2D)$ then one has $\frac{1}{2} < r_0 < 1$ and*

$$(3.5) \quad S_r^{out}(S^{in}, D) = \begin{cases} \lambda(D/(1-r)) & \text{if } 0 \leq r \leq 1-r_0 \\ S^{in} & \text{if } 1-r_0 \leq r \leq r_0 \\ S_2^*(S^{in}, D, r) & \text{if } r_0 \leq r \leq 1. \end{cases}$$

- 3) *If $\lambda(2D) \leq S^{in}$ then one has $0 < r_0 \leq \frac{1}{2}$ and*

$$(3.6) \quad S_r^{out}(S^{in}, D) = \begin{cases} \lambda(D/(1-r)) & \text{if } 0 \leq r \leq r_0 \\ S_2^*(S^{in}, D, r) & \text{if } r_0 \leq r \leq 1. \end{cases}$$

Proof. The proof is given in Appendix B.5. □

For a deeper analysis, we consider the functions $D \mapsto S_r^{out}(S^{in}, D)$ and $D \mapsto S^{out}(S^{in}, D)$ where we fix the input substrate density S^{in} and the parameter r . We add the following assumption, which is satisfied by concave growth functions and also by Hill functions as it is shown in Section 5.

Assumption 3. *For every $r \in (0, 1)$, the function $D \in (0, rm) \mapsto g_r(D) \in \mathbb{R}$ is strictly increasing.*

We have the following result:

Proposition 3. *Assume that Assumptions 1 and 3 are satisfied. For any $r \in (0, 1)$ and $S^{in} > 0$, there exists a critical value $D_r = D_r(S^{in})$, which is the unique solution of the implicit equation $S^{in} = g_r(D)$, such that the serial configuration of two interconnected chemostats is more efficient than a simple chemostat if and only if $0 < D < D_r(S^{in})$. That is to say, for any $0 < D < D_r(S^{in})$, one has $S_r^{out}(S^{in}, D) < S^{out}(S^{in}, D)$.*

Proof. The proof is given in Appendix B.6. □

The result of Proposition 3 is illustrated by Figure 3. In this Figure, the critical value $D_r = D_r(S^{in})$ is depicted for various values of r and S^{in} , illustrating then Proposition 1 which asserts that, for a fixed dilution rate D , the output substrate concentration decreases

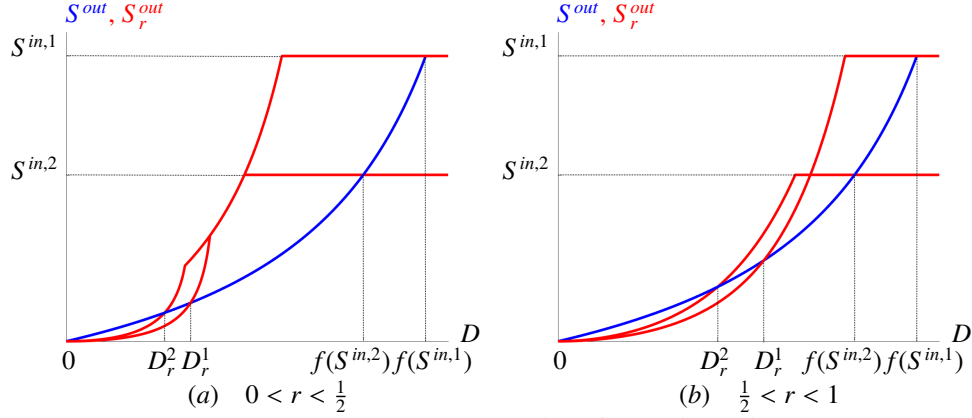


FIGURE 3. The output substrate concentration of the serial device and the simple chemostat are respectively represented by the red and the blue curves. D_r^i is the implicit solution of $S^{in,i} = g_r(D)$, $i = 1, 2$. The output substrate concentration of the serial device (in red) decreases as S^{in} increases.

when S^{in} increases.

The following Lemmas 3 and 4 provide sufficient conditions for Assumption 2 and 3 to be satisfied. These conditions are useful for the applications given in Section 5. For this purpose, we consider the function γ defined by

$$(3.7) \quad \gamma(r, D) := g_r(D) \quad \text{where} \quad \text{dom}(\gamma) = \{(r, D) : 0 < r < 1, 0 < D < rm\},$$

which consists simply in considering $g_r(D)$, given by (3.3), as a function of both variables r and D . If $\frac{\partial \gamma}{\partial r}(r, D) < 0$ for all $(r, D) \in \text{dom}(\gamma)$, then Assumption 2 is satisfied. Similarly, if $\frac{\partial \gamma}{\partial D}(r, D) > 0$ for all $(r, D) \in \text{dom}(\gamma)$, then Assumption 3 is satisfied. The following lemmas give equivalent conditions, and also sufficient conditions, for partial derivatives of γ to have their signs as indicated above.

Lemma 3. For $D \in (0, m)$, let l_D be defined on $(D/m, 1]$ by $l_D(r) = \lambda(D/r)$. The following conditions are equivalent

- (1) For all $(r, D) \in \text{dom}(\gamma)$, $\frac{\partial \gamma}{\partial r}(r, D) < 0$.
- (2) For all $D \in (0, m)$ and $r \in (D/m, 1)$, $l_D(1) > l_D(r) + (1 - r)l'_D(r)$.

If l_D is strictly convex on $(D/m, 1]$, then the condition 2 is satisfied. If, in addition, f is twice derivable, then l_D is twice derivable and the following conditions are equivalent

- (3) For all $D \in (0, m)$ and $r \in (D/m, 1]$, $l'_D(r) > 0$.
- (4) For all $S > 0$, $f(S)f''(S) < 2(f'(S))^2$.

Proof. The proof is given in Appendix D.1. □

Lemma 4. The following conditions are equivalent

- (1) For all $(r, D) \in \text{dom}(\gamma)$, $\frac{\partial \gamma}{\partial D}(r, D) > 0$.
- (2) For all $(r, D) \in \text{dom}(\gamma)$, $f'(\lambda(D/r)) < f'(\lambda(D))/r^2$.

If f' is decreasing, then the condition 2 is satisfied.

Proof. The proof is given in Appendix D.2. □

Remark 3. *If the growth function is twice derivable and satisfies $f''(S) \leq 0$ for all $S > 0$, then the condition 4 in Lemma 3 and the condition 2 in Lemma 4 are satisfied. Thus, Assumptions 2 and 3 are satisfied. Therefore, our results apply for concave growth functions. The previous lemmas allow to consider a non-concave growth function such as the Hill function as shown in Section 5.3.*

3.2. Biomass productivity. Let us consider the dependency of the productivity of the biomass with respect to the dilution rate D and the input concentration S^{in} . Recall that for a simple chemostat the output biomass at steady state is given by $x^{out} = S^{in} - S^{out}$. Thus, the productivity of a single chemostat is defined by

$$(3.8) \quad P(S^{in}, D) := Qx^{out}(S^{in}, D) = \begin{cases} 0 & \text{if } D \geq f(S^{in}) \\ VD(S^{in} - \lambda(D)) & \text{if } D < f(S^{in}). \end{cases}$$

Let $D^{opt}(S^{in})$ be the dilution rate which maximizes $P(S^{in}, D)$ i.e.

$$(3.9) \quad D^{opt}(S^{in}) := \operatorname{argmax}_{0 \leq D \leq f(S^{in})} P(S^{in}, D).$$

Assumption 4. *The dilution rate $D^{opt}(S^{in})$ defined by (3.9) is unique.*

Proposition 4. *The dilution rate $D^{opt}(S^{in})$ defined by (3.9) is the solution of equation $S^{in} = g(D)$ where g is defined by (3.4).*

Proof. The proof is given in Appendix C.1. □

The productivity of the two serial interconnected chemostats at steady-state is defined as

$$(3.10) \quad P_r(S^{in}, D) := Qx_r^{out}(S^{in}, D)$$

with $x_r^{out} = S^{in} - S_r^{out}$. Using the definitions (3.1) and (3.2) of $S_r^{out}(S^{in}, D)$, for $r \in (0, 1)$ we have

$$(3.11) \quad P_r(S^{in}, D) = \begin{cases} 0 & \text{if } \max\{r, 1-r\}f(S^{in}) \leq D \\ VD(S^{in} - \lambda(D/(1-r))) & \text{if } rf(S^{in}) \leq D \leq (1-r)f(S^{in}) \\ VD(S^{in} - S_2^*(S^{in}, D, r)) & \text{if } D < rf(S^{in}) \end{cases}$$

and $P_r(S^{in}, D) = P(S^{in}, D)$, when $r = 0$ and $r = 1$. As a consequence of Theorem 3 we obtain the following result.

Corollary 1. *Assume that Assumptions 1 and 2 are satisfied.*

- *If $S^{in} \leq g(D)$ then for any $r \in (0, 1)$, $P_r(S^{in}, D) < P(S^{in}, D)$.*
- *If $S^{in} > g(D)$ then $P_r(S^{in}, D) > P(S^{in}, D)$ if and only if $r \in (r_1, 1)$, where $r_1 = r_1(S^{in}, D)$ is the unique solution of $S^{in} = g_r(D)$*

and $P_r(S^{in}, D) = P(S^{in}, D)$ for $r = 0$, $r = r_1$ and $r = 1$.

Proof. The proof is given in Appendix C.2. □

This Corollary ensures that if $S^{in} > g(D)$ and for any $r_1 < r < 1$, the productivity of the biomass of the serial configuration is larger than the one of the simple chemostat. These conditions, related to the productivity of the biomass, are the same conditions that arose in the case of the minimization of the output substrate concentration, see Section 3.1. We illustrate this Corollary in Section 4 in Figure 8.

3.3. Biogas flow rate. Let us consider the dependency of the biogas flow rate with respect to the dilution rate D and the input concentration S^{in} . Recall that for a simple chemostat the output biomass at steady state is given by $x^{out} = S^{in} - S^{out}$. Classically, the biogas flow rate at steady-state of the simple chemostat model is defined as

$$(3.12) \quad G(S^{in}, D) := Vx^{out}f(S^{out}) = \begin{cases} 0 & \text{if } D \geq f(S^{in}) \\ VD(S^{in} - \lambda(D)) & \text{if } D < f(S^{in}). \end{cases}$$

The biogas flow rate of the serial configuration of two chemostats is the sum with the same propositional coefficient kept equal to one, which is thus defined as

$$(3.13) \quad G_r(S^{in}, D) := \sum_{i=1}^2 V_i x^{out,i} f(S^{out,i}).$$

with V_i the volume, $x^{out,i}$ the output steady-state biomass and $S^{out,i}$ the output steady-state substrate concentration, all corresponding to the tank $i = 1, 2$. In this respect, for $r = 0$ and $r = 1$ we have $G_r(S^{in}, D) = G(S^{in}, D)$ and when $r \in (0, 1)$ it is formulated by

$$(3.14) \quad G_r(S^{in}, D) = \begin{cases} 0 & \text{if } \max\{r, 1-r\}f(S^{in}) \leq D \\ VD(S^{in} - \lambda(D/(1-r))) & \text{if } rf(S^{in}) \leq D \leq (1-r)f(S^{in}) \\ VD(S^{in} - \lambda(D/r)) + \\ V(1-r)f(S_2^*)(S^{in} - S_2^*) & \text{if } D < rf(S^{in}). \end{cases}$$

Proposition 5. For any $D \in [0, m)$, $S^{in} > 0$ and $r \in (0, 1)$, one has $G_r(S^{in}, D) = P_r(S^{in}, D)$.

Proof. The proof is given in Appendix C.3. □

We know that for a single chemostat, the biogas flow rate and the productivity of the biomass at steady state are identical. Proposition 5 asserts this same conclusion in the case of two serial interconnected chemostats. Thereby, we deduce that analyzing the productivity of the biomass or the biogas flow rate at the steady state of two interconnected chemostats are equivalent. In this respect, Corollary 1 and the following result are verified for both performance criteria.

Proposition 6. Let $S^{in} > 0$. Let $G^{max}(S^{in}) := \max_{D \in (0, f(S^{in}))} G(S^{in}, D)$. For any $D > 0$ and $r \in (0, 1)$, one has $G_r(S^{in}, D) < G^{max}(S^{in})$.

Proof. The proof is given in Appendix C.4. □

The two functions $D \mapsto G_r(S^{in}, D)$ and $D \mapsto G(S^{in}, D)$ are depicted in Figure 4. It shows that, for fixed values S^{in} and r , the biogas production of the serial configuration of two chemostats is more efficient than the one of the single chemostat if and only if $0 < D < D_r$ with D_r solution of $S^{in} = g_r(D)$, as it was proved in Proposition 3. In addition, Proposition 6 guarantees that the biogas flow rate of the serial device will never exceed the maximal biogas flow rate of the single chemostat. In other words, the extrema of the blue curve of the serial configuration will never exceed the extremum of the black curve of the simple chemostat.

This result has been graphically shown in [12] and [20] for the productivity of the biomass in the particular case of the Monod growth function. The simulations depicted in these references predicted that spatialization as we proposed it, does not give a better productivity of the biomass than a simple chemostat. According to Proposition 5, we know that at steady-state, the biogas flow rate and the productivity of the biomass are the same, which explains why predictions of the authors of [12] and [20] correspond to Proposition 6.

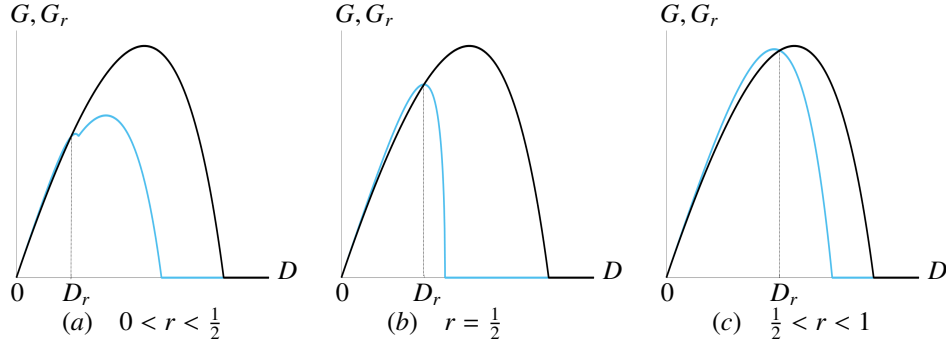


FIGURE 4. The biogas flow rate of the serial configuration of two chemostats (in light blue) and the one of the single chemostat (in black).

4. OPERATING DIAGRAM

The operating diagram is the bifurcation diagram for which the values of the biological parameters are fixed. The various regions of the operating diagram reflect qualitatively different dynamics. The operating parameters which are the input concentration S^{in} and the dilution rate D of the chemostat can be chosen by the practitioners and the behavior of the model is discussed with respect to them. In contrast, the biological parameters are the ones of the growth function since they depend on the organisms, the substrates and the conversion rate Y , and are usually estimated in the laboratory.

Let the curves Φ_r and Φ_{1-r} in the (S^{in}, D) positive plane be defined by

$$(4.1) \quad \Phi_r := \{(S^{in}, D) : D = rf(S^{in})\} \quad \text{and} \quad \Phi_{1-r} := \{(S^{in}, D) : D = (1-r)f(S^{in})\}.$$

The curves Φ_r and Φ_{1-r} split the positive plane (S^{in}, D) in several regions denoted $I_0(r)$, $I_1(r)$, $I_2(r)$ and $I_3(r)$ defined by:

$$\begin{aligned} I_0(r) &:= \{(S^{in}, D) : \max\{r, 1-r\}f(S^{in}) \leq D\}, \\ I_1(r) &:= \{(S^{in}, D) : rf(S^{in}) \leq D < (1-r)f(S^{in})\}, 0 \leq r < \frac{1}{2}, \\ I_2(r) &:= \{(S^{in}, D) : 0 < D < \min\{r, 1-r\}f(S^{in})\}, \\ I_3(r) &:= \{(S^{in}, D) : (1-r)f(S^{in}) \leq D < rf(S^{in})\}, \frac{1}{2} < r \leq 1. \end{aligned}$$

We fix r in $(0, 1)$ and we depict in the plane (S^{in}, D) the regions in which the solution of system (2.6), with positive initial condition, globally converges towards one of the steady states E_0 , E_1 or E_2 . In the case $0 \leq r < \frac{1}{2}$ [res. $\frac{1}{2} < r \leq 1$], the regions $I_0(r)$, $I_1(r)$ and $I_2(r)$ [res. $I_0(r)$, $I_2(r)$ and $I_3(r)$] form a partition of the positive plane. The region $I_1(r)$ for $\frac{1}{2} \leq r \leq 1$ [res. $I_3(r)$ for $0 \leq r \leq \frac{1}{2}$] is empty. The behavior of the system in each region is given in Table 1.

Let the curve Γ_r in the positive plane (S^{in}, D) be defined by

$$(4.2) \quad \Gamma_r := \{(S^{in}, D) : S^{in} = g_r(D)\}$$

with g_r defined by (3.3).

Lemma 5. For all $r \in (0, 1)$ the curve Φ_r defined by (4.1) is always above the curve Γ_r defined by (4.2) in the plane (S^{in}, D) .

Proof. The proof is given in Appendix D.3. □

	$I_0(r)$	$I_1(r)$	$I_2(r)$	$I_3(r)$
E_0	GAS	U	U	U
E_1		GAS	U	
E_2			GAS	GAS

TABLE 1. Stability of the steady states in the various regions of the operating diagram. The letter U means that the steady state is unstable. The letters GAS mean that the steady state is globally asymptotically stable in the positive orthant. No letter means that the steady state does not exist.

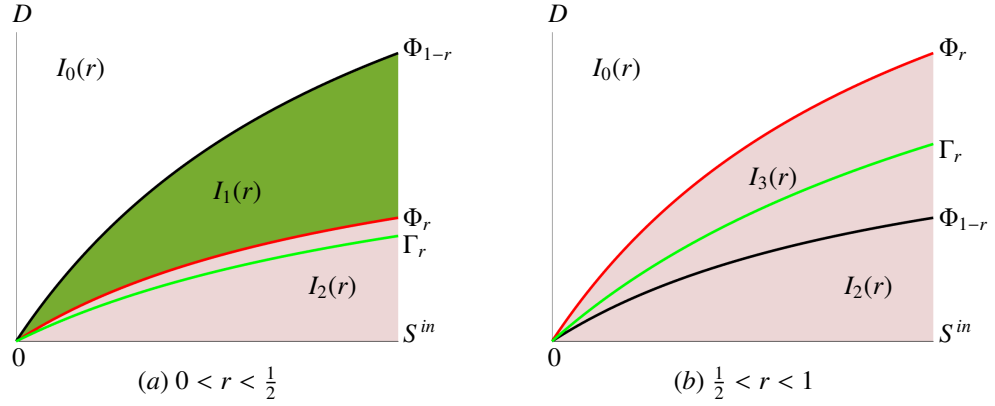


FIGURE 5. The operating diagram of two interconnected chemostats in serial depending on the parameter r .

In this respect, for any growth function f verifying Assumption 1, the operating diagram of system (2.6) looks like Figure 5. Thus, according to Theorem 2, for the minimization of the output substrate concentration criterion, the serial configuration is more efficient than the simple chemostat if and only if $S^{in} > g_r(D)$ i.e. if and only if (S^{in}, D) is strictly below the curve Γ_r , see Figure 5. Let us use the operating plane to give a better understanding of the results of Proposition 2 on the behavior of the function $r \mapsto S_r^{out}(S^{in}, D)$, according to (S^{in}, D) . To this end, we consider the curves Φ_1 , Γ and $\Phi_{1/2}$ in the operating plane defined by:

$$(4.3) \quad \Phi_{1/2} := \{(S^{in}, D) : S^{in} = \lambda(2D)\}, \quad \Phi_1 := \{(S^{in}, D) : S^{in} = \lambda(D)\}$$

$$(4.4) \quad \text{and} \quad \Gamma := \{(S^{in}, D) : S^{in} = g(D)\}$$

with g defined by (3.4).

Curves Γ and $\Phi_{1/2}$ lie below curve Φ_1 . Therefore, curves Γ , $\Phi_{1/2}$ and Φ_1 split the operating plane into at most five regions defined by:

$$(4.5) \quad \begin{aligned} J_0 &:= \{(S^{in}, D) : S^{in} \leq \lambda(D)\}, \\ J_1 &:= \{(S^{in}, D) : \lambda(D) < S^{in} \leq \min(g(D), \lambda(2D))\}, \\ J_2 &:= \{(S^{in}, D) : g(D) < S^{in} < \lambda(2D)\}, \\ J_3 &:= \{(S^{in}, D) : \max(g(D), \lambda(2D)) \leq S^{in}\}, \\ J_4 &:= \{(S^{in}, D) : \lambda(2D) < S^{in} < g(D)\}. \end{aligned}$$

These regions are shown in Figure 6 which is given for an illustrative example but does not correspond to any particular growth function. Regions J_0 , J_1 and J_3 always exist and

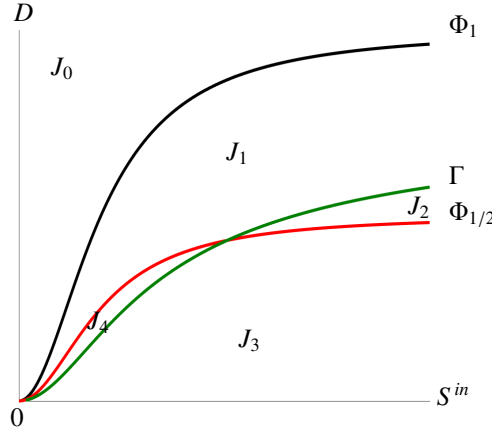


FIGURE 6. Regions in the operating plan with different behaviors of the mapping $r \mapsto S_r^{out}(S^{in}, D)$ where (S^{in}, D) is fixed.

are connected. However, regions J_2 and J_4 do not necessarily exist and if they exist, in general, they are not necessarily connected, depending on the relative positions of curves Γ and $\Phi_{1/2}$. For instance, for linear growth rates, $\Gamma = \Phi_{1/2}$ and regions J_2 and J_4 do not exist (see Section 5.1); for Monod growth function, curve Γ is above curve $\Phi_{1/2}$ and region J_4 does not exist (see Section 5.2); for Hill growth function, regions J_2 and J_4 both exist (see Section 5.3) and are connected. Notice that for plotting operating diagrams we must choose the growth function f and the values of the biological parameters, see Figures 9 and 14. We can state now the main result on function $r \mapsto S_r^{out}(S^{in}, D)$, for $(S^{in}, D) \in J_i$, $i = 0, \dots, 4$.

Proposition 7. *Let J_i , $i = 0, 1, \dots, 4$ be defined by (4.5). The behavior of function $r \mapsto S_r^{out}(S^{in}, D)$, according to (S^{in}, D) is as follows:*

- If $(S^{in}, D) \in J_0$ then, for all $r \in [0, 1]$, $S_r^{out}(S^{in}, D) = S^{out}(S^{in}, D) = S^{in}$.
- If $(S^{in}, D) \in J_1$ then, when $\lambda(D) < S^{in} < \lambda(2D)$, $S_r^{out}(S^{in}, D)$ is given by (3.5) and when $S^{in} = \lambda(2D)$, $S_r^{out}(S^{in}, D)$ is given by (3.6). In addition, for all $r \in (0, 1)$, $S_r^{out}(S^{in}, D) > S^{out}(S^{in}, D)$. The equality is fulfilled for $r = 0$ and $r = 1$, see Figure 7 (a).

- If $(S^{in}, D) \in J_2$ then $S_r^{out}(S^{in}, D)$ is given by (3.5) and $S_r^{out}(S^{in}, D) < S^{out}(S^{in}, D)$ if and only if $r \in (r_1, 1)$ where $r_1 = r_1(S^{in}, D)$ is the unique solution of $S^{in} = g_r(D)$. The equality is fulfilled for $r = 0$, $r = r_1$ and $r = 1$, see Figure 7 (b).
- If $(S^{in}, D) \in J_3$ then $S_r^{out}(S^{in}, D)$ is given by (3.6) and $S_r^{out}(S^{in}, D) < S^{out}(S^{in}, D)$ if and only if $S^{in} > g(D)$ and $r \in (r_1, 1)$ where $r_1 = r_1(S^{in}, D)$ is the unique solution of $S^{in} = g_r(D)$. The equality is fulfilled for $r = 0$, $r = r_1$ and $r = 1$, see Figure 7 (c).
- If $(S^{in}, D) \in J_4$ then $S_r^{out}(S^{in}, D)$ is given by (3.6) and for all $r \in (0, 1)$, $S_r^{out}(S^{in}, D) > S^{out}(S^{in}, D)$. The equality is fulfilled for $r = 0$ and $r = 1$, see Figure 7 (d).

Proof. The proof is given in Appendix B.7 □

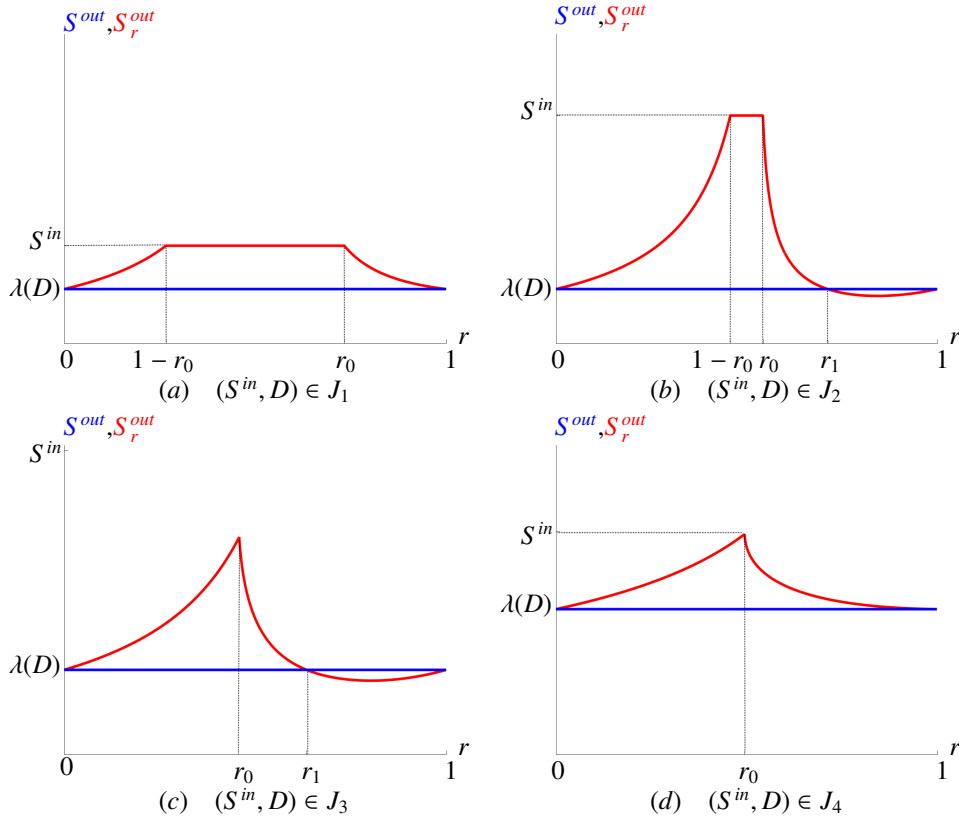


FIGURE 7. The map $r \mapsto S_r^{out}(S^{in}, D)$ (in red) in the regions J_1 , J_2 , J_3 and J_4 compared to $r \mapsto S^{out}(S^{in}, D)$ (in blue). The value r_1 is the unique solution of $S^{in} = g_r(D)$ and $r_0 = D/f(S^{in})$.

According to the regions depicted in Figure 6, we obtain Figure 7 which covers the whole possible cases of the behavior of the function $r \mapsto S_r^{out}(S^{in}, D)$. Thusly, we can minimize the output substrate concentration at the steady state by using a serial configuration of two interconnected chemostats instead of one chemostat if (S^{in}, D) is fixed in the regions J_2 or J_3 (i.e. $S^{in} > g(D)$) and for $r_1 < r < 1$.

We have previously shown that Corollary 1 is a consequence of Theorem 3 and one can see in Proof C.2 of Corollary 1 that comparing the two quantities $P_r(S^{in}, D)$ and $P(S^{in}, D)$

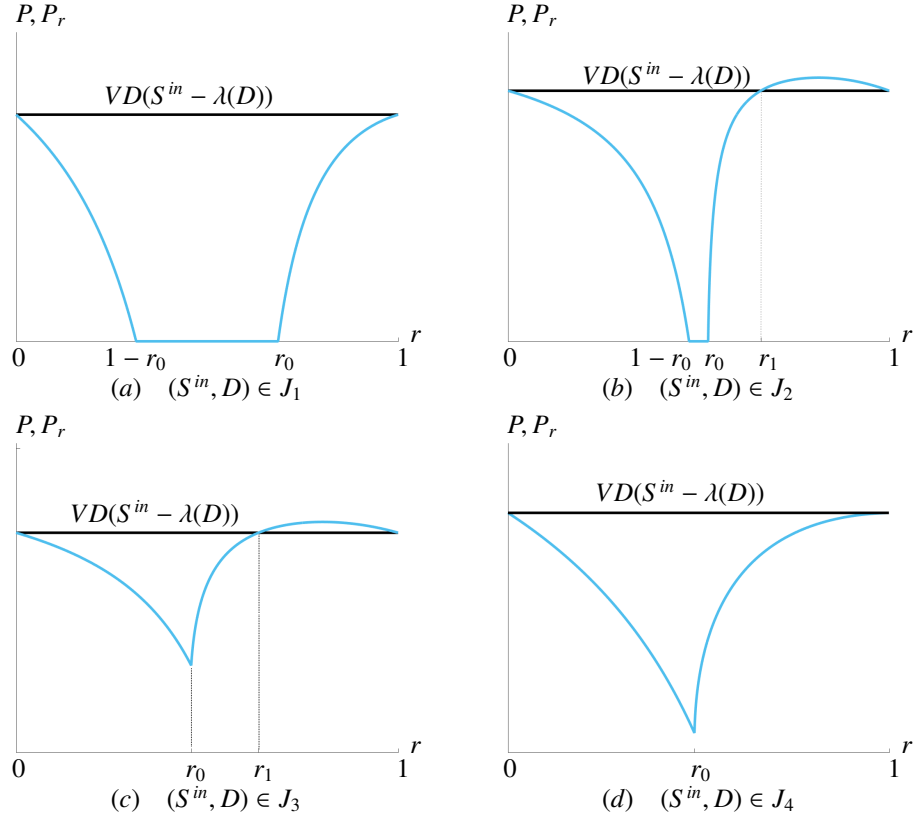


FIGURE 8. The map $r \mapsto P_r(S^{in}, D)$ (in light blue) in the regions J_1 , J_2 , J_3 and J_4 compared to $r \mapsto P(S^{in}, D)$ (in black). The value r_1 is the unique solution of $S^{in} = g_r(D)$ and $r_0 = D/f(S^{in})$.

involves the comparison of the two quantities $S_r^{out}(S^{in}, D)$ and $S^{out}(S^{in}, D)$. That is why, the curves representing the productivity of the biomass depicted in Figure 8 are analogous to the curves of Figure 7. In Figure 8, we fix $r \in (0, 1)$ and we plot the functions $r \mapsto P_r(S^{in}, D)$ and $r \mapsto P(S^{in}, D)$ for (S^{in}, D) fixed in the regions J_1 , J_2 , J_3 and J_4 . As in the case of the output substrate concentration, it is shown that the productivity of the biomass or the biogas flow rate of the serial configuration is larger than the one of the simple chemostat if and only if $r \in (r_1, 1)$ and (S^{in}, D) is fixed in one of the regions J_2 or J_3 .

5. APPLICATIONS AND NUMERICAL ILLUSTRATIONS

In this section, we consider three different kinetics: the linear function, the Monod function and the Hill function. Table 2 gives the analytical expressions of most of the results previously presented. These expressions show that an analytical study of the different performance criteria is possible.

5.1. Linear function. We consider f as a linear function defined by $f(S) = aS$. According to Table 2, remark that $\lambda(2D) = g(D)$ then, the curves $\Phi_{1/2}$ and Γ defined respectively by (4.3) and (4.4) merge and constitute only one curve. The behavior of the maps

Functions	$g_r(D)$	$g(D)$	$\lambda(2D)$
$f(S) = aS, a > 0$	$\frac{D(1+r)}{ar}$	$\frac{2D}{a}$	$\frac{2D}{a}$
$f(S) = \frac{mS}{K+S}$	$\frac{DK(m(1+r)-D)}{(m-D)(mr-D)}$	$\frac{KD(2m-D)}{(m-D)^2}$	$\frac{2KD}{m-2D}$
$f(S) = \frac{mS^2}{K^2+S^2}$	$\frac{K\sqrt{D}}{1-r} \left(\frac{1}{\sqrt{rm-D}} - \frac{r}{\sqrt{m-D}} \right)$	$\frac{K}{2} \sqrt{\frac{D}{(m-D)^3}} (3m-2D)$	$K \sqrt{\frac{2D}{m-2D}}$

TABLE 2. Analytical expressions obtained for a linear, Monod and Hill (with $p = 2$) growth functions.

$r \mapsto S_r^{out}(S^{in}, D)$ and $r \mapsto S^{out}(S^{in}, D)$ or $r \mapsto P_r(S^{in}, D)$ and $r \mapsto P(S^{in}, D)$ depends on the position of (S^{in}, D) in the three regions $J_i, i = 0, 1, 3$ represented in Figure 9 (a). These regions are defined by

$$J_0 = \{(S^{in}, D) : S^{in} \leq \lambda(D)\}, J_1 = \{(S^{in}, D) : \lambda(D) < S^{in} \leq \lambda(2D)\}, J_3 = \{(S^{in}, D) : \lambda(2D) \leq S^{in}\}.$$

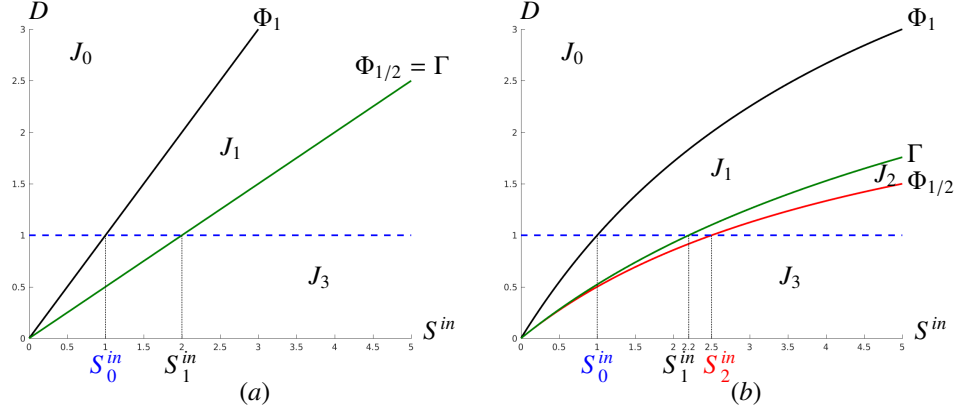


FIGURE 9. Regions in the operating plane with f defined by $f(S) = S$ in (a) and $f(S) = 6S/(5+S)$ in (b). The dashed blue line $D = 1$ indicates the respective critical values S_0^{in}, S_1^{in} and S_2^{in} of Figures 10 and 11.

For a fixed value of D , the passageway from the region J_0 to J_1 is defined by the critical value $S_0^{in} = \lambda(D)$ and the passageway from the region J_1 to J_3 is defined by the critical value $S_1^{in} = g(D) = \lambda(2D)$ as shown in Figures 9 (a) and 10 (b). As stated in Lemma 2, for any $S^{in} > S_1^{in}$ there exists a threshold $r_1 = r_1(S^{in}, D)$ solution of $S^{in} = g_r(D)$ which is explicitly given by

$$(5.1) \quad r_1(S^{in}, D) = \frac{D}{aS^{in} - D}.$$

Then, according to the three performance criteria which are the minimization of the output substrate concentration, the maximization of the productivity of the biomass and the maximization of the biogas flow rate, the serial configuration is more efficient than the simple chemostat if and only if $S^{in} > S_1^{in}$ and $r \in (r_1, 1)$. This result is illustrated in Figure 10 for minimization of the output substrate concentration criterion. Figure 10 (a) should be compared with Figure 6 of [16], where the part of the curves represented in Figure 10 (a)

corresponding to $r > r_0$, for which $S_r^{out}(S^{in}, D) = S_2^*(S^{in}, D, r)$, are depicted. Indeed, in [16], the authors were only interested in the case where the positive equilibrium E_2 is GAS. The threshold $S_1^{in} = 2$ shown in Figure 6 of [16] is given by $S_1^{in} = g(1)$ and for any $S^{in} > 2$ the threshold $r_1(S^{in}, D)$ is explicitly given by (5.1).

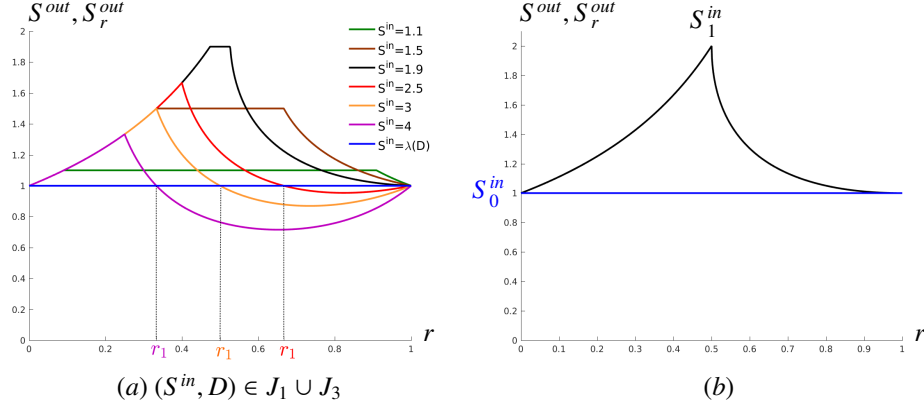


FIGURE 10. (a): The function $r \mapsto S_r^{out}(S^{in}, D)$ with $f(S) = S$, $D = 1$, $r_1(4, 1) = 0.333$, $r_1(3, 1) = 0.5$ and $r_1(2.5, 1) = 0.666$. (b): For $D = 1$, the critical values corresponding to the passageways between the regions J_i , $i = 0, 1, 3$ are $S_0^{in} = 1$ and $S_1^{in} = 2$.

5.2. Monod function. The Monod function is given by $f(S) = mS/(K + S)$, see the second line of Table 2.

Lemma 6. *The curve Γ is located strictly above the curve $\Phi_{1/2}$ in the (S^{in}, D) plane.*

Proof. The proof is given in the Appendix D.4 □

Thus, considering a Monod function induces four regions J_i , $i = 0, 1, 2, 3$ in the operating plane, that describe the behaviors of the maps $r \mapsto S_r^{out}(S^{in}, D)$ and $r \mapsto P_r(S^{in}, D)$, which depend on the position of (S^{in}, D) in these regions, as depicted in Figure 9 (b). The behavior of the map $r \mapsto S_r^{out}(S^{in}, D)$ through these regions is depicted in Figure 11 (a). For a fixed dilution rate D , the limit curves Φ_1 , Γ and $\Phi_{1/2}$ define critical values denoted $S_0^{in} = \lambda(D)$, $S_1^{in} = g(D)$ and $S_2^{in} = \lambda(2D)$, that respectively characterize the passageways between the regions J_i , $i = 0, 1, 2, 3$, see Figures 9 (b) and 11 (b). As stated in Lemma 2, for any $S^{in} > S_1^{in}$ there exists a threshold $r_1 = r_1(S^{in}, D)$ solution of $S^{in} = g_r(D)$ which is explicitly given by

$$(5.2) \quad r_1(S^{in}, D) = \frac{D(K + S^{in})(m - D)}{m(S^{in}m - D(K + S^{in}))}.$$

Then, according to the three studied performance criteria, the serial configuration is more efficient than the simple chemostat if and only if $S^{in} > S_1^{in}$ and $r_1 < r < 1$. Figure 11 (a) should be compared with Figure 9 of [16], where the part of the curves represented in Figure 11 (a) corresponding to $r > r_0$, for which $S_r^{out}(S^{in}, D) = S_2^*(S^{in}, D, r)$, are depicted. Indeed, in [16], the authors were only interested to the case where the positive equilibrium E_2 is GAS. If $D = 1$ as shown in Figure 9 (b), the threshold S_1^{in} is given by $S_1^{in} = g(1) = 2.2$ and for any $S^{in} > 2.2$ the threshold r_1 is explicitly given by (5.2).

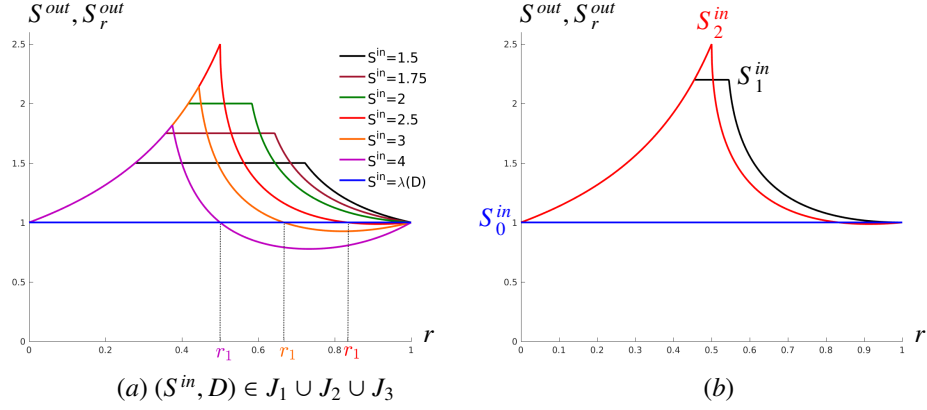


FIGURE 11. (a): The function $r \mapsto S_r^{out}(S^{in}, D)$ with $f(S) = 6S/(5 + S)$, $D = 1$, $r_1(4, 1) = 0.5$, $r_1(3, 1) = 0.666$ and $r_1(2.5, 1) = 0.833$. (b): The critical values corresponding to the passageways between the regions J_i , $i = 0, 1, 2, 3$ are $S_0^{in} = 1$, $S_1^{in} = 2.2$ and $S_2^{in} = 2.5$.

Notice that Figures 10 (a) and 11 (a) illustrate Proposition 1. As stated in this Proposition, when D is fixed, one can remark that when increasing S^{in} , the output substrate concentration at the steady state decreases. Thus, the minimum of the curve $r \mapsto S_r^{out}(S^{in}, D)$, representing the optimal point that gives the best possible serial configuration, decreases as $S^{in} > S_1^{in} = g(D)$ and S^{in} increases.

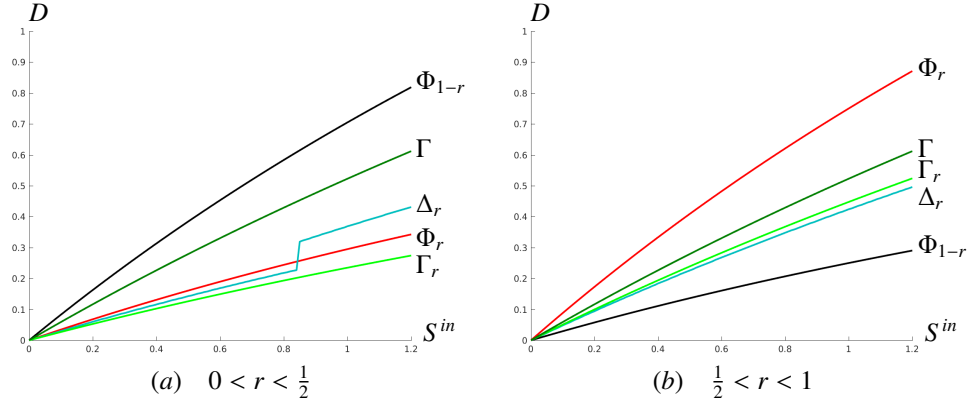


FIGURE 12. The curves Φ_r and Φ_{1-r} are defined by (4.1). The curves Γ_r and Γ are respectively defined by (4.2) and (4.4). The curve Δ_r of maximal productivity, defined by (5.3), is obtained numerically with $f(S) = 6S/(5 + S)$, $V = 1$, and (a): $r = 0.295$, (b): $r = 0.75$.

For the purpose of comparing the productivity of the biomass of both configurations, for a fixed $r \in (0, 1)$, we characterize the operating parameters (S^{in}, D) that allow the optimal biomass productivity of the serial configuration. Let Δ_r be the curve defined by

$$(5.3) \quad \Delta_r := \left\{ (S^{in}, D_r^{opt}(S^{in})) : D_r^{opt}(S^{in}) = \operatorname{argmax}_{0 \leq D \leq f(S^{in})} P_r(S^{in}, D) \right\}.$$

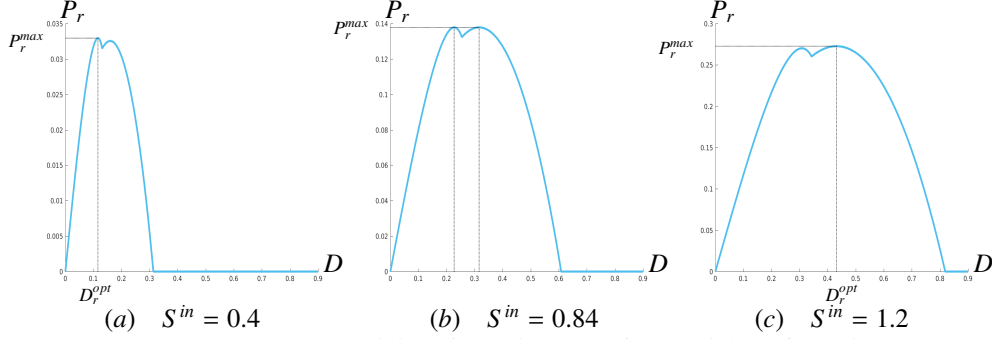


FIGURE 13. The productivity of the biomass, of the serial configuration with $D_r^{opt} = D_r^{opt}(S^{in})$ defined in (5.3) and $P_r^{max} = P_r(S^{in}, D_r^{opt})$, corresponding to the Figure 12 (a).

where P_r is defined by (3.11). This curve is obtained numerically and depicted in the operating plane (S^{in}, D) , see Figure 12 (a) and (b). For the values of the parameters used in Figure 12 (a), corresponding to the case $0 < r < 1/2$, there exists a threshold $S^{in} \approx 0.84$ such that for $0 < S^{in} < 0.84$, the maximum of $P_r(S^{in}, D)$ is reached when $P_r(S^{in}, D) = VD(S^{in} - S_2^*(S^{in}, D, r))$, and for $S^{in} > 0.84$, it is reached when $P_r(S^{in}, D) = VD(S^{in} - \lambda(D/(1-r)))$, as shown in Figure 13. Therefore, for $0 < S^{in} < 0.84$, the maximum of $P_r(S^{in}, D)$ is reached when E_2 is stable, i.e. when $D < rf(S^{in})$, as illustrated for $S^{in} = 0.4$ in Figure 13 (a). That is why, for $0 < S^{in} < 0.84$, the curve Δ_r is strictly below the curve Φ_r . In contrast, for $S^{in} > 0.84$ the maximum of $P_r(S^{in}, D)$ is reached when E_1 is stable, i.e. when $D \geq rf(S^{in})$, as illustrated for $S^{in} = 1.2$ in Figure 13 (c). That is why, for $S^{in} > 0.84$, the curve Δ_r is strictly above the curve Φ_r . In the limit case $S^{in} = 0.84$, both maxima of $P_r(S^{in}, D)$ are equal, as shown in Figure 13 (b). This corresponds to the leap of the curve Δ_r , shown in Figure 12 (a). On the other hand, for $1/2 < r < 1$, the equilibrium E_1 cannot be stable and $P_r(S^{in}, D) = VD(S^{in} - S_2^*(S^{in}, D, r))$, whenever it is positive. Therefore, its maximum is reached when the positive equilibrium E_2 is stable, that is why, the curve Δ_r is strictly below the curve Φ_r , see Figure 12 (b).

According to Proposition 4, Γ is the curve of equation $D = D^{opt}(S^{in})$, where $D^{opt}(S^{in})$ is defined in (3.9). In other words, $D^{opt}(S^{in})$ is the optimal dilution rate corresponding to the maximal productivity of the biomass, of the simple chemostat. We observe on Figure 12 that Δ_r is strictly below the curve Γ . Hence $D^{opt}(S^{in}) > D_r^{opt}(S^{in})$, as it was also depicted in Figure 4. We conjecture that this property is always verified.

5.3. Hill function. For all $p > 1$, the non-concave Hill function is given by $f(S) = mS^p/(K^p + S^p)$.

Proposition 8. *The Hill function verifies Assumptions 2 and 3.*

Proof. The proof is given in Appendix D.5 □

Proposition 8 shows that we can use effectively a non-concave growth function in our analysis. In the following, we consider the case where $p = 2$, see third line of Table 2.

Lemma 7. *Let us denote $D_1 := m(3 - \sqrt{5})/4$.*

If $0 < D < D_1$ then the curve $\Phi_{1/2}$ defined by (4.3) is strictly above the curve Γ defined in (4.4). In contrast, if $D_1 < D < \frac{m}{2}$ then the curve $\Phi_{1/2}$ is strictly below the curve Γ .

Proof. The proof is given in Appendix D.6 \square

According to Lemma 7, considering an Hill function with $p = 2$ induces five regions $J_i, i = 0, 1, 2, 3, 4$ in the operating plane, defined in (4.5), that describe the behavior of the maps $r \mapsto S_r^{out}(S^{in}, D)$ and $r \mapsto S^{out}(S^{in}, D)$ or $r \mapsto P_r(S^{in}, D)$ and $r \mapsto P(S^{in}, D)$, which depends on the position of (S^{in}, D) in these regions (see Figure 14). For a fixed dilution rate D , the limit curves Φ_1, Γ and $\Phi_{1/2}$ define critical values denoted $S_0^{in} = \lambda(D), S_1^{in} = g(D)$ and $S_2^{in} = \lambda(2D)$ that characterize the passageways between the different regions $J_i, i = 0, 1, 2, 3, 4$. Notice that, if $D < D_1$, as shown in Figure 14 (b), where D_1 is defined in Lemma 7 then, we have $S_1^{in} > S_2^{in}$ and the behavior of the maps $r \mapsto S_r^{out}(S^{in}, D)$ is as depicted in Figure 15 (b). Remark that, in this case, the region where $S_r^{out}(S^{in}, D) = S^{in}$ disappears before the emergence of the threshold r_1 solution of $S^{in} = g_r(D)$, that is, before the emergence of the region where the serial configuration is more efficient than the simple chemostat i.e. $S_r^{out}(S^{in}, D) < S^{out}(S^{in}, D)$. On the other hand, if $D > D_1$, as shown in Figure 14 (a) then, we have $S_1^{in} < S_2^{in}$ and the behavior of the maps $r \mapsto S_r^{out}(S^{in}, D)$ is as depicted in Figure 15 (a).

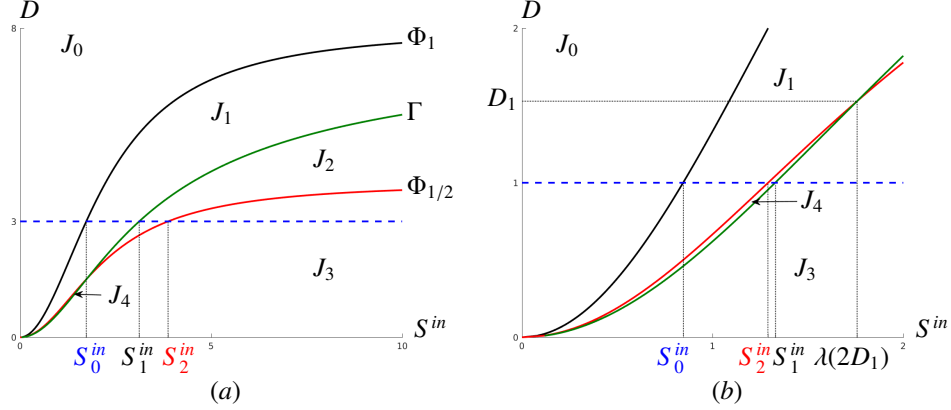


FIGURE 14. The five regions in the operating plane where $f(S) = 8S^2/(5 + S^2)$. The blue dashed lines $D = 3$ and $D = 1$ indicate respectively the critical values S_0^{in}, S_1^{in} and S_2^{in} , of schemes (a) and (b) of Figure 15.

As stated in Lemma 2, for any $S^{in} > S_1^{in}$, there exists a threshold $r_1 = r_1(S^{in}, D)$ solution of $S^{in} = g_r(D)$ such that, for $r_1 < r < 1$, the performance of the serial configuration is more efficient than the one of the simple chemostat. In other words, the output substrate concentration at steady-state of the serial configuration is lesser than the one of the simple chemostat if and only if $(S^{in}, D) \in J_2 \cup J_3$ and $r \in (r_1, 1)$.

6. CONCLUSION

This work presents an in-depth mathematical study of a model of two serial interconnected chemostats with one species and a monotonic growth function. We analyze, at steady-state, three different performance criteria: the minimization of the output substrate concentration, the maximization of the productivity of the biomass and the maximization of the biogas flow rate. The aim is to compare with the performance of the single chemostat. A part of this paper extends some of the results published in [16] and presented in the thesis [21]. In these both references, the concavity of the function f is a required assumption but this assumption is not necessary in our analysis. The thorough study of our

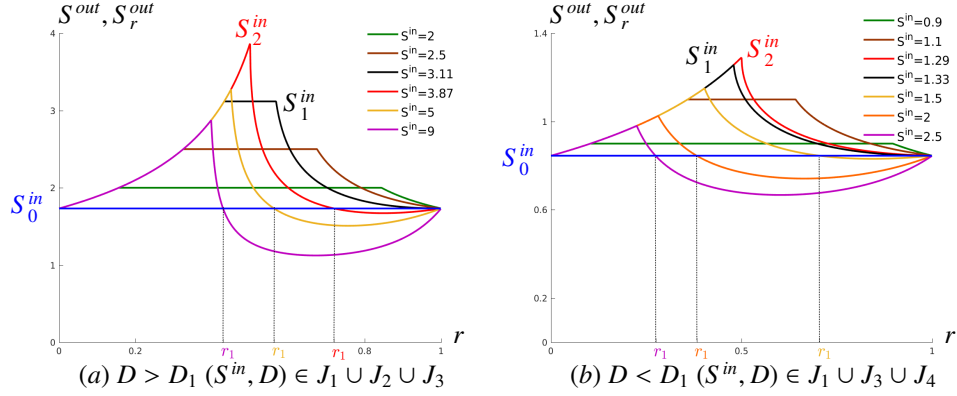


FIGURE 15. The function $r \rightarrow S_r^{out}(S^{in}, D)$ with $f(S) = 8S^2/(\sqrt{5} + S^2)$ and $D_1 = 1.5279$. (a): $D = 3$, $r_1(9, 3) = 0.43$, $r_1(5, 3) = 0.56$, $r_1(3.87, 3) = 0.72$, $S_0^{in} = 1.73$, $S_1^{in} = 3.11$ and $S_2^{in} = 3.87$. (b): $D = 1$, $r_1(2.5, 1) = 0.28$, $r_1(2, 1) = 0.38$, $r_1(1.5, 1) = 0.70$, $S_0^{in} = 0.85$, $S_1^{in} = 1.33$ and $S_2^{in} = 1.29$.

model reveals three main results. First, we provide an explicit expression depending on the dilution rate D , that represents the threshold $S_1^{in} = g(D)$ on the input concentration for the performance. We deduce that there exists a configuration of two tanks that is better than a single tank. Actually, through the optimization of the distribution of the volume V and the threshold S_1^{in} , we distinguish which configuration is the best. Secondly, we infer that maximizing the production of the biomass is equivalent to maximize the biogas flow rate at steady-state even in the case of a serial device of two interconnected chemostats. At the end, we obtain the same conditions for the three performance criteria. Thus, reducing the output substrate concentration, maximizing the production of the biomass or maximizing the biogas flow rate at steady state involve the same conditions and the same threshold S_1^{in} . These conditions are necessary and sufficient to allow the best performance, and they are characterized by the input concentration S^{in} , the dilution rate D and the parameter r . Finally, for deeper understanding, we depict the corresponding operating diagram of the model which describes the behavior of the steady states. This diagram presents the conditions which induce an optimal configuration with regions characterized by the parameter r and the operating parameters S^{in} and D .

To broaden and deepen the present work, a forthcoming paper will present the analysis of performance, of an extension, of the model of two serial interconnected chemostats, with death rates. This future work will also include a comparison with the simple chemostat with death rate.

APPENDIX A. PROOF OF THEOREM 1

A.1. Existence of equilibria. System (2.6) has a cascade structure. Let us consider $z_i(t) = S_i(t) + x_i(t)$ ($i = 1, 2$) then, we have the following system

$$(A.1) \quad \begin{aligned} \dot{z}_1 &= \frac{D}{r} (S^{in} - z_1) \\ \dot{x}_1 &= -\frac{D}{r} x_1 + f(z_1 - x_1)x_1 \\ \dot{z}_2 &= \frac{D}{1-r} (z_1 - z_2) \\ \dot{x}_2 &= \frac{D}{1-r} (x_1 - x_2) + f(z_2 - x_2)x_2. \end{aligned}$$

One can easily show that $\lim_{t \rightarrow +\infty} z_i(t) = S^{in}$ ($i = 1, 2$). Therefore $(x_1(t), x_2(t))$ satisfies an asymptotically autonomous dynamics, whose limiting system

$$(A.2) \quad \begin{aligned} \dot{x}_1 &= -\frac{D}{r}x_1 + f(S^{in} - x_1)x_1 \\ \dot{x}_2 &= \frac{D}{1-r}(x_1 - x_2) + f(S^{in} - x_2)x_2 \end{aligned}$$

is defined in the square $\Sigma := [0, S^{in}] \times [0, S^{in}]$. System (A.2) has a cascade structure. It admits at most three equilibria:

$$e_0 := (0, 0), \quad e_1 := (0, S^{in} - \lambda(D/(1-r))) \quad \text{and} \quad e_2 := (S^{in} - \lambda(D/r), x_2^*)$$

with $x_2^* \in (0, S^{in})$ a solution, if it exists, of equation

$$(A.3) \quad \varphi(x_2) = S^{in} - \lambda(D/r) \quad \text{with} \quad \varphi(x_2) := x_2 - (1-r)D^{-1}f(S^{in} - x_2)x_2.$$

The equilibria E_0, E_1 and E_2 of (2.6) corresponding to e_0, e_1 and e_2 , respectively, have the same values $x_i, i = 1, 2$, and their corresponding S_i are given by $S_i = S^{in} - x_i, i = 1, 2$. Note that e_0, e_1 and e_2 give

$$(S_1, S_2) = (S^{in}, S^{in}), \quad (S_1, S_2) = (S^{in}, \lambda(D/(1-r))) \quad \text{and} \quad (S_1, S_2) = (\lambda(D/r), S_2^*),$$

where $S_2^* = S^{in} - x_2^*$. This proves that one has $\bar{S}_2 = \lambda(D/(1-r))$ and $S_1^* = \lambda(D/r)$ as stated in the Theorem. The equilibrium e_0 , and hence the corresponding equilibrium E_0 , always exists. The equilibrium e_1 , exists if and only if $S^{in} - \lambda(D/(1-r)) > 0$, that is $D < (1-r)f(S^{in})$, which is the condition of existence of E_1 in the Theorem. For the existence and uniqueness of e_2 , note that x_2^* is a solution of (A.3), if and only if $S_2^* = S^{in} - x_2^*$ satisfies $f(S_2^*) = h(S_2^*)$, which proves (2.9). The function h is positive, strictly decreasing and $h(S_1^*) = 0$, where $S_1^* = \lambda(D/r)$, if and only if $S^{in} > \lambda(D/r)$, see Figure 2. Thus, as f is strictly increasing (see Assumption 1), there exists a unique solution of $h(S_2) = f(S_2)$ denoted S_2^* in $[0, S_1^*)$. Therefore, the equilibrium e_2 exists if and only if $S^{in} > \lambda(D/r)$, that is $D < rf(S^{in})$, which is the condition of existence of E_2 in the statement of the Theorem.

A.2. Local stability. For the local stability, the Jacobian matrix associated to system (A.2) is defined by

$$J := \begin{pmatrix} -D/r + f(S^{in} - x_1) - f'(S^{in} - x_1)x_1 & 0 \\ D/(1-r) & -D/(1-r) + f(S^{in} - x_2) - f'(S^{in} - x_2)x_2 \end{pmatrix}$$

The eigenvalues of this triangular matrix are its diagonal elements. For e_0 , the eigenvalues are $-D/r + f(S^{in})$ and $-D/(1-r) + f(S^{in})$. Therefore e_0 , and hence E_0 , is LES if and only if $D > \max\{r, 1-r\}f(S^{in})$. For e_1 , the eigenvalues are $-D/r + f(S^{in})$ and $-f'(\lambda(D/(1-r)))(S^{in} - \lambda(D/(1-r)))$. The second eigenvalue is negative if and only if $D < (1-r)f(S^{in})$, that is, e_1 exists. Therefore e_1 , and hence E_1 , is LES if and only if $rf(S^{in}) < D < (1-r)f(S^{in})$. For e_2 , the eigenvalues are $-f'(\lambda(D/r))(S^{in} - \lambda(D/r))$ and $-D/(1-r) + f(S_2^*) - f'(S_2^*)x_2^*$, where $x_2^* = S^{in} - S_2^*$, and S_2^* is the solution of equation (2.9). As it is seen in Figure 2 (a), $0 < S_2^* < S_1^* < S^{in}$. Hence $(S_1^* - S_2^*)/(S^{in} - S_2^*) < 1$. Thus, we have $h(S_2^*) < D/(1-r)$ and, according to (2.9), this is equivalent to $f(S_2^*) < D/(1-r)$. Consequently, the second eigenvalue is negative, which proves that e_2 , and hence E_2 , is LES, if and only if the first eigenvalue is negative. This condition is equivalent to $S^{in} > \lambda(D/r)$, i.e $D < rf(S^{in})$, which is the condition of existence of E_2 .

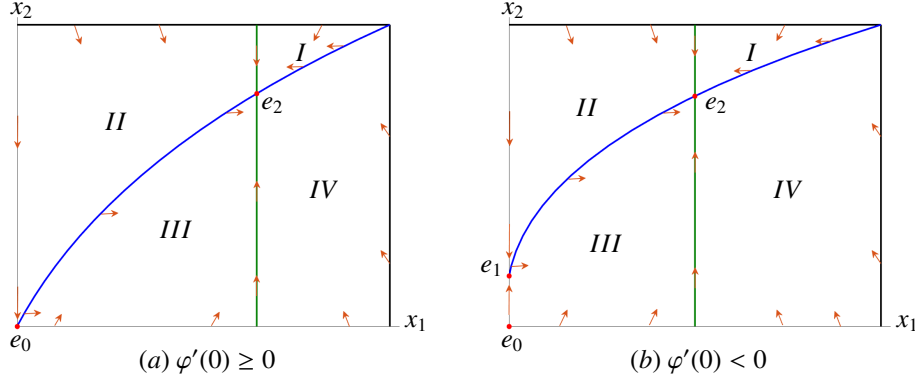


FIGURE 16. Global stability of the equilibrium e_2 . (a): e_1 does not exist. (b) e_1 exists.

A.3. Global stability. For the global asymptotic stability we use phase plane arguments, as in the proof of Proposition 7 in [22], or in Section 2.1.2.3 of [4]. We give the details of the proof when e_2 exists. The case where e_2 does not exist but e_1 exists and the case where neither e_2 nor e_1 exist are similar. The isoclines $x_1 = S^{in} - \lambda(D/r)$ and $x_1 = \varphi(x_2)$, where φ is defined by (A.3), separate the interior of Σ into four regions defined by

$$I : \dot{x}_1 < 0, \dot{x}_2 < 0, \quad II : \dot{x}_1 > 0, \dot{x}_2 < 0, \quad III : \dot{x}_1 > 0, \dot{x}_2 > 0, \quad IV : \dot{x}_1 < 0, \dot{x}_2 > 0.$$

Two cases must be distinguished, according to the existence, or not of e_1 , see Figure 16. We consider the case where e_1 exists. The case where it does not exist is similar. The isocline $x_1 = \varphi(x_2)$ is as shown in Figure 16 (b), that is, it is the graph of a strictly increasing function. Indeed, using the definition (A.3) of φ , we have

$$\varphi'(x_2) = 1 - \frac{1-r}{D} f(S^{in} - x_2) + \frac{1-r}{D} f'(S^{in} - x_2)x_2.$$

Note that $\varphi'(0) = 1 - \frac{1-r}{D} f(S^{in})$. Therefore, e_1 exists if and only if $\varphi'(0) < 0$ as shown in the figure. For $x_2 \in (\bar{x}_2, S^{in})$, where $\bar{x}_2 = S^{in} - \lambda(D/(1-r))$ is the x_2 component of e_1 , we have

$$\varphi'(x_2) > 1 - \frac{1-r}{D} f(S^{in} - x_2) > 1 - \frac{1-r}{D} f(S^{in} - \bar{x}_2) = 0,$$

which proves that φ is strictly increasing. The vector field associated to (A.2) is horizontal if $x_1 = \varphi(x_2)$ and vertical if $x_1 = 0$ or $x_1 = S^{in} - \lambda(D/r)$. It is directed as shown in the Figure. Assume first that $(x_1(0), x_2(0)) \in I \cup III$. These regions are positively invariant. Since in I [resp. III], $x_1(t)$ and $x_2(t)$ are strictly decreasing [resp. increasing], the following limits exist:

$$(A.4) \quad \lim_{t \rightarrow +\infty} x_1(t) = x_{1\infty}, \quad \lim_{t \rightarrow +\infty} x_2(t) = x_{2\infty}.$$

Therefore, $(x_{1\infty}, x_{2\infty})$ is an equilibrium of (A.2), which belongs to the closure \bar{I} or the closure \bar{III} . Since e_0, e_1 and e_2 (resp. e_2) are the only steady states in \bar{III} (resp. \bar{I}) and, since e_1 attracts only solution with $x_1(0) = 0$ and e_0 attracts no solutions with positive initial conditions, it follows that

$$(A.5) \quad e_2 = (x_{1\infty}, x_{2\infty}).$$

Assume now that $(x_1(0), x_2(0)) \in IV$. If $(x_1(t), x_2(t))$ remains in IV for all $t > 0$ then $x_1(\cdot)$ is strictly decreasing and $x_2(\cdot)$ is strictly increasing. Thus, the limits (A.4) exist. Hence,

$(x_{1\infty}, x_{2\infty})$ is an equilibrium of (A.2), which belongs to the closure \overline{IV} . Since e_2 is the only equilibrium in \overline{IV} , we conclude that (A.5) holds. If $(x_1(t), x_2(t))$ leaves the region IV , then it can only enter in the region I . Hence, as shown previously it necessarily tends to e_2 and hence, (A.5) holds. The same argument shows that any solution starting with initial condition in II always remains in II and then converges to e_2 or leaves the region II , then enters necessarily in region III , and then, as shown previously it tends to e_2 . Therefore e_2 is GAS in the interior of Σ . Using the theory of asymptotically autonomous systems (see Appendix F in [6]), we deduce that E_2 is GAS if and only if it exists.

APPENDIX B. OUTPUT SUBSTRATE CONCENTRATION

B.1. Proof of Proposition 1. Let $S_2^{*i} = S_2^*(S^{in,i}, D, r)$, $i = 1, 2$. Suppose that $S_2^{*1} \geq S_2^{*2}$. Since f is increasing then, we have $f(S_2^{*1}) \geq f(S_2^{*2})$. Since $f(S_2^{*1}) = h_1(S_2^{*1})$ and $f(S_2^{*2}) = h_2(S_2^{*2})$ then, we have $h_1(S_2^{*1}) \geq h_2(S_2^{*2})$. Since $h_2 > h_1$ then, we have $h_2(S_2^{*2}) > h_1(S_2^{*2})$. Since h_1 is decreasing then, we have $h_1(S_2^{*2}) \geq h_1(S_2^{*1})$. Therefore, we have $h_1(S_2^{*1}) > h_1(S_2^{*1})$ which is a contradiction. Hence $S_2^{*1} < S_2^{*2}$.

B.2. Proof of Theorem 2. Recall that $S_2^*(S^{in}, D, r)$ is the unique solution of equation (2.9). Let us first prove that

$$(B.1) \quad S_2^*(S^{in}, D, r) < \lambda(D) \quad \text{if and only if} \quad S^{in} > g_r(D).$$

Since f is strictly increasing and h is strictly decreasing then, $S_2^*(S^{in}, D, r) < \lambda(D)$ is equivalent to $h(\lambda(D)) < f(\lambda(D)) = D$. Thus, using the definition of h , the condition $h(\lambda(D)) < D$ is written as

$$\frac{D(\lambda(D/r) - \lambda(D))}{(1-r)(S^{in} - \lambda(D))} < D,$$

which is equivalent to $S^{in} > \lambda(D) + (\lambda(D/r) - \lambda(D))/(1-r)$. Hence, according to the definition (3.3) of g_r , this is equivalent to $S^{in} > g_r(D)$. Notice also that the function g_r , defined by (3.3), satisfies

$$(B.2) \quad g_r(D) = \lambda(D/r) + \frac{r(\lambda(D/r) - \lambda(D))}{1-r}.$$

Therefore, one has $g_r(D) > \lambda(D/r)$.

Let us go now to the proof of the Theorem. Assume that $S^{in} > g_r(D)$. Then, $S^{in} > \lambda(D/r) > \lambda(D)$, so that, as shown by (2.5) and (3.1), we have

$$(B.3) \quad S_r^{out}(S^{in}, D) = S_2^*(S^{in}, D, r) \quad \text{and} \quad S^{out}(S^{in}, D) = \lambda(D).$$

Therefore, using (B.1), we have $S_r^{out}(S^{in}, D) < S^{out}(S^{in}, D)$. Assume now that $S^{in} \leq g_r(D)$. When $r < 1/2$, three cases must be distinguished. First, if $\lambda(D) < \lambda(D/r) < S^{in} \leq g_r(D)$, then, by (2.5) and (3.1), we obtain (B.3). Hence, using (B.1), we have $S_r^{out}(S^{in}, D) \geq S^{out}(S^{in}, D)$. Secondly, if $\lambda(D) < \lambda(D/(1-r)) < S^{in} \leq \lambda(D/r)$ then, by (2.5) and (3.1), $S_r^{out}(S^{in}, D) = \lambda(D/(1-r))$ and $S^{out}(S^{in}, D) = \lambda(D)$. Therefore, we have $S_r^{out}(S^{in}, D) > S^{out}(S^{in}, D)$. Finally, if $S^{in} \leq \lambda(D)$, then $S_r^{out}(S^{in}, D) = S^{out}(S^{in}, D) = S^{in}$. When $r \geq 1/2$, the proof is similar, excepted that we must distinguish only two cases, $\lambda(D) < S^{in} \leq \lambda(D/r)$ and $S^{in} \leq \lambda(D)$.

In conclusion, for any $r \in (0, 1)$, $S_r^{out}(S^{in}, D) < S^{out}(S^{in}, D)$ if and only if $S^{in} > g_r(D)$.

B.3. Proof of Lemma 2. Let $D < m$. From Assumption 2, the function $r \in (D/m, 1) \mapsto g_r(D)$ is strictly decreasing. From Assumption 1, we have $\lim_{r \rightarrow D/m} \lambda(D/r) = \lambda(m) = +\infty$. Thus, $\lim_{r \rightarrow D/m} g_r(D) = +\infty$. Using L'Hôpital's rule, one has $\lim_{r \rightarrow 1} g_r(D) = g(D)$. Then, using Intermediate Value Theorem, we deduce that for $S^{in} > g(D)$ there exists a unique $r_1 = r_1(S^{in}, D)$ in $(0, 1)$ such that $S^{in} = g_{r_1}(D)$. Since the function $r \mapsto g_r(D)$ is strictly decreasing then, $r > r_1(S^{in}, D)$ if and only if $S^{in} = g_{r_1}(D) > g_r(D)$ which ends the proof of the Lemma.

B.4. Proof of Theorem 3.

- From Assumptions 1 and 2, the function $r \in (D/m, 1) \mapsto g_r(D)$ is strictly decreasing. Thus, for any $r \in (0, 1)$, $g(D) < g_r(D)$. If $S^{in} \leq g(D)$ then $S^{in} < g_r(D)$ and according to Theorem 2 we deduce that $S_r^{out}(S^{in}, D) > S^{out}(S^{in}, D)$.
- If $S^{in} > g(D)$ then according to Lemma 2, there exists a unique $r_1 = r_1(S^{in}, D)$ in $(0, 1)$ such that $S^{in} = g_{r_1}(D)$, where for all $r > r_1$, we have $S^{in} > g_r(D)$. Thus, according to Theorem 2 we deduce that $S_r^{out}(S^{in}, D) < S^{out}(S^{in}, D)$.

The equality in the limiting cases $r = 0$ and $r = 1$ is already verified, see (3.2).

If $r = r_1$ then $S^{in} = g_{r_1}(D)$. According to (B.2), one has $\lambda(D/r_1) < g_{r_1}(D)$, that is, $\lambda(D/r_1) < S^{in}$. Thus, one has $S_{r_1}^{out}(S^{in}, D) = S_2^*(S^{in}, D, r_1)$ where $S_2^*(S^{in}, D, r_1)$ is the unique solution of $h(S_2)|_{r=r_1} = f(S_2)$. Consequently, one has $S_2^*(S^{in}, D, r_1) = \lambda(D)$ if and only if $h(\lambda(D))|_{r=r_1} = f(\lambda(D))$, which is equivalent to

$$D(\lambda(D/r_1) - \lambda(D)) / ((S^{in} - \lambda(D))(1 - r_1)) = D,$$

that is, $\lambda(D/r_1) - \lambda(D) = (1 - r_1)(S^{in} - \lambda(D))$. Consequently, one obtains that $\lambda(D) + (\lambda(D/r_1) - \lambda(D)) / (1 - r_1) = S^{in}$, which is equivalent to $g_{r_1}(D) = S^{in}$. This ends the proof of the Theorem.

B.5. Proof of Proposition 2. Let us consider $r_0 = D/f(S^{in})$ i.e. $S^{in} = \lambda(D/r_0)$.

1) When $S^{in} \leq \lambda(D)$ one has, for all $r \in (0, 1)$, $\lambda(D) \leq \min\{\lambda(D/(1-r)), \lambda(D/r)\}$ i.e. $S^{in} \leq \min\{\lambda(D/(1-r)), \lambda(D/r)\}$. Then, according to (3.1) one has $S_r^{out}(S^{in}, D) = S^{in}$.

2) When $\lambda(D) < S^{in} < \lambda(2D)$, one has $r_0 \in (1/2, 1)$. Firstly, if $0 \leq r \leq 1 - r_0$ then, one has $\lambda(D/(1-r)) \leq \lambda(D/r_0) \leq \lambda(D/r)$ i.e. $\lambda(D/(1-r)) \leq S^{in} \leq \lambda(D/r)$. This is equivalent to $rf(S^{in}) \leq D \leq (1-r)f(S^{in})$. According to (3.1), one has $S_r^{out}(S^{in}, D) = \lambda(D/(1-r))$. Secondly, if $1 - r_0 \leq r \leq r_0$, one has $\lambda(D/r_0) \leq \min\{\lambda(D/(1-r)), \lambda(D/r)\}$ i.e. $S^{in} \leq \min\{\lambda(D/(1-r)), \lambda(D/r)\}$. According to (3.1), one has $S_r^{out}(S^{in}, D) = S^{in}$. Finally, if $r_0 < r \leq 1$, one has $\lambda(D/r) \leq \lambda(D/r_0)$ i.e. $\lambda(D/r) \leq S^{in}$ then, according to (3.1), one has $S_r^{out}(S^{in}, D) = S_2^*(S^{in}, D, r)$. These all prove (3.5).

3) When $\lambda(2D) \leq S^{in}$ one has $r_0 \in (0, 1/2]$. If $0 \leq r \leq r_0$ then $\lambda(D/(1-r)) \leq \lambda(D/r_0) \leq \lambda(D/r)$ i.e. $\lambda(D/(1-r)) \leq S^{in} \leq \lambda(D/r)$. According to (3.1), one has $S_r^{out}(S^{in}, D) = \lambda(D/(1-r))$. If $r_0 \leq r \leq 1$ then $\lambda(D/r) \leq \lambda(D/r_0)$ i.e. $\lambda(D/r) \leq S^{in}$. According to (3.1), one has $S_r^{out}(S^{in}, D) = S_2^*(S^{in}, D, r)$. These all prove (3.6).

B.6. Proof of Proposition 3. Let $r \in (0, 1)$. From Assumption 3, the function $D \in [0, rm) \mapsto g_r(D)$ is strictly increasing. From Assumption 1, we have $\lim_{D \rightarrow rm} \lambda(D/r) = \lambda(m) = +\infty$. Thus, $\lim_{D \rightarrow 0} g_r(D) = +\infty$ and $g_r(0) = 0$. Then, using Intermediate Value Theorem, we deduce that for $S^{in} > 0$ there exists a unique $D_r = D_r(S^{in})$ in $[0, rm)$ such that $S^{in} = g_r(D_r)$. Since the function $D \mapsto g_r(D)$ is strictly increasing then, $0 < D < D_r(S^{in})$ if and only if $0 < g_r(D) < g_r(D_r) = S^{in}$. Consequently, according to Theorem 2, $g_r(D) < S^{in}$ if and only if $S_r^{out}(S^{in}, D) < S^{out}(S^{in}, D)$ which ends the proof of the Proposition.

B.7. Proof of Proposition 7. The result is a direct consequence of Proposition 2 and Theorem 3. We give the details for regions J_1 and J_2 . The proof for other regions is similar.

If $(S^{in}, D) \in J_1$ then, according to (4.5), $\lambda(D) < S^{in} \leq \min(g(D), \lambda(2D))$. Therefore, $\lambda(D) < S^{in} \leq \lambda(2D)$. When $\lambda(D) < S^{in} < \lambda(2D)$, from Proposition 2, $S_r^{out}(S^{in}, D)$ is given by (3.5) and if $S^{in} = \lambda(2D)$ then $S_r^{out}(S^{in}, D)$ is given by (3.6). Now, using $S^{in} \leq g(D)$, from Theorem 3, we have for all $r \in (0, 1)$, $S_r^{out}(S^{in}, D) > S^{out}(S^{in}, D)$.

If $(S^{in}, D) \in J_2$ then, according to (4.5), $g(D) < S^{in} < \lambda(2D)$. Therefore, $\lambda(D) < S^{in} < \lambda(2D)$ and from Proposition 2, $S_r^{out}(S^{in}, D)$ is given by (3.5). Now, using $g(D) < S^{in}$, from Lemma 2, there exists a threshold r_1 , defined as the unique solution of $S^{in} = g_r(D)$. Therefore, from Theorem 3, $S_r^{out}(S^{in}, D) < S^{out}(S^{in}, D)$ if and only if $r \in (r_1, 1)$ and equality holds if and only if $r = 0$, $r = r_1$ or $r = 1$.

APPENDIX C. PRODUCTIVITY AND BIOGAS PRODUCTION

C.1. Proof of Proposition 4. The equation $P(S^{in}, D) = 0$ admits the two roots $D = 0$ and $D = f(S^{in})$. For all $D > 0$, $P(S^{in}, D)$ is positive if and only if $S^{in} > \lambda(D)$. In addition, for all $D < f(S^{in})$ we have

$$\frac{\partial P}{\partial D}(S^{in}, D) = V \left(S^{in} - \lambda(D) - \frac{D}{f'(\lambda(D))} \right) = V(S^{in} - g(D))$$

with g defined by (3.4). Thus, $\frac{\partial P}{\partial D}(S^{in}, D) = 0$ is verified if and only if $S^{in} = g(D)$. Consequently, using Assumption 4, D^{opt} defined in (3.9) is the unique solution of $S^{in} = g(D)$.

C.2. Proof of Corollary 1. One knows that $x_r^{out}(S^{in}, D) = S^{in} - S_r^{out}(S^{in}, D)$ and $x^{out}(S^{in}, D) = S^{in} - S^{out}(S^{in}, D)$. Firstly, if $S^{in} \leq g(D)$ then according to Theorem 3, for any $r \in (0, 1)$, one has $S_r^{out}(S^{in}, D) > S^{out}(S^{in}, D)$. Thus, for any $r \in (0, 1)$, one has $x_r^{out}(S^{in}, D) < x^{out}(S^{in}, D)$. Consequently, for any $r \in (0, 1)$, one has $P_r(S^{in}, D) < P(S^{in}, D)$. Secondly, if $S^{in} > g(D)$ then according to Theorem 3, one has $S_r^{out}(S^{in}, D) < S^{out}(S^{in}, D)$ if and only if $r_1 < r < 1$ with r_1 defined in Lemma 2. Then, one has $x_r^{out}(S^{in}, D) > x^{out}(S^{in}, D)$ if and only if $r_1 < r < 1$. Consequently, one has $P_r(S^{in}, D) > P(S^{in}, D)$ if and only if $r_1 < r < 1$. Finally, if $r = 0$, $r = r_1$ or $r = 1$, then one has $S_r^{out}(S^{in}, D) = S^{out}(S^{in}, D)$. Thus, for $r = 0, r_1, 1$ one has $x_r^{out}(S^{in}, D) = x^{out}(S^{in}, D)$. Consequently, if $r = 0, r = r_1$ or $r = 1$ then, $P_r(S^{in}, D) = P(S^{in}, D)$, which ends the proof of the Corollary.

C.3. Proof of Proposition 5. Let V be a fixed volume. In the following, we use the respective definitions (3.11) and (3.14) of P_r and G_r . In both cases: $\max\{r, 1-r\}f(S^{in}) \leq D$ and $rf(S^{in}) \leq D \leq (1-r)f(S^{in})$, it is clear that $G_r(S^{in}, D) = P_r(S^{in}, D)$. In addition, if $D < rf(S^{in})$ then

$$G_r(S^{in}, D) = VD(S^{in} - \lambda(D/r)) + V(1-r)f(S_2^*)(S^{in} - S_2^*)$$

with S_2^* the unique solution of (2.9). According to this equation, G_r can be written as

$$G_r(S^{in}, D) = VD(S^{in} - \lambda(D/r)) + VD(\lambda(D/r) - S_2^*).$$

Thus, we deduce that $G_r(S^{in}, D) = P_r(S^{in}, D) = VD(S^{in} - S_2^*)$ and consequently, for any $r \in (0, 1)$, we have $G_r(S^{in}, D) = P_r(S^{in}, D)$.

C.4. Proof of Proposition 6. Let V be a fixed volume and $S^{in} > 0$. Let us consider the function $\varphi(S) = f(S)(S^{in} - S)$. Considering the change of variable $S = \lambda(D)$, one can easily verify that $\varphi'(S) = 0$ is equivalent to $S^{in} - g(D) = 0$. According to Assumption 4, φ admits a unique maximum. We maximize the biogas flow rate at steady-state with respect to D . On the one hand, the biogas flow rate of the simple chemostat is defined by $G(S^{in}, D) = V\varphi(S^{out}(D))$ with S^{out} defined by (2.5). Then, the maximal biogas flow rate of the simple chemostat is $G^{max}(S^{in}) = V \max_{D \in (0, f(S^{in}))} \varphi(S^{out}(D))$. Since the map λ defines a homeomorphism from $[0, f(S^{in})]$ to $[0, S^{in}]$ then $\max_{D \in (0, f(S^{in}))} \varphi(S^{out}(D)) = \max_{S \in (0, S^{in})} \varphi(S)$. On the other hand, as $S_1^* > S_2^*$ and using the definition (3.13) of G_r , the biogas flow rate of the two serial interconnected chemostats at steady-state is defined by $G_r(S^{in}, D) = rV\varphi(S_1^*) + (1-r)V\varphi(S_2^*)$ with $S_1^* = \lambda(D/r)$ and S_2^* the unique solution of (2.9). In addition, as for all $D < f(S^{in})$ we have $\varphi(S_i^*(D)) < \max_{S \in (0, S^{in})} \varphi(S)$, $i = 1, 2$ then, we have

$$G_r(S^{in}, D) < rV \max_{S \in (0, S^{in})} \varphi(S) + (1-r)V \max_{S \in (0, S^{in})} \varphi(S).$$

Hence, we deduce that $G_r(S^{in}, D) < V \max_{S \in (0, S^{in})} \varphi(S)$ which is equivalent to $G_r(S^{in}, D) < G^{max}(S^{in})$. This completes the proof of the Proposition.

APPENDIX D. TECHNICAL RESULTS

D.1. Proof of Lemma 3. Using $l_D(r) = \lambda(D/r)$, $\gamma(r, D) = g_r(D)$, defined by (3.3), is given by

$$\gamma(r, D) = l_D(1) + \frac{l_D(r) - l_D(1)}{1-r}$$

The partial derivative, with respect to r of γ is given then by

$$\frac{\partial \gamma}{\partial r}(r, D) = \frac{l_D'(r)(1-r) + l_D(r) - l_D(1)}{(1-r)^2}.$$

Therefore, $\frac{\partial \gamma}{\partial r}(r, D) < 0$ if and only if $l_D(1) > l_D(r) + (1-r)l_D'(r)$, which proves the equivalence of conditions 1 and 2 of the Lemma.

Moreover, if l_D is strictly convex on $(D/m, 1]$ then for all s and r in $(D/m, 1]$, if $s \neq r$, then

$$l_D(s) > l_D(r) + (s-r)l_D'(r).$$

Taking $s = 1$ and $r \in (D/m, 1)$ one obtains the condition 2.

Assume now that f , and hence l_D , are twice derivable. Using $\lambda'(D) = 1/f'(\lambda(D))$ and $\lambda''(D) = -f''(\lambda(D))/(f'(\lambda(D)))^3$, we can write

$$l_D''(r) = \frac{2D}{r^3} \lambda'(D/r) + \frac{D^2}{r^4} \lambda''(D/r) = \frac{D}{r^3 (f'(\lambda(D/r)))^3} \left(2(f'(\lambda(D/r)))^2 - (D/r)f''(\lambda(D/r)) \right)$$

Therefore, the condition 3 is equivalent to the following condition:

$$(D.1) \quad \text{For all } D \in (0, rm) \text{ and } r \in (D/m, 1], Df''(\lambda(D/r))/r < 2(f'(\lambda(D/r)))^2$$

Using the notation $S = \lambda(D/r)$, which is the same as $f(S) = D/r$, the condition (D.1) is equivalent to : for all $S > 0$, $f(S)f''(S) < 2(f'(S))^2$, which is the condition 4 in the Lemma.

D.2. Proof of Lemma 4. Using $\lambda'(D) = 1/f'(\lambda(D))$, the partial derivative, with respect to D of $\gamma(r, D) = g_r(D)$, defined by (3.3), is given by

$$\frac{\partial \gamma}{\partial D}(r, D) = \lambda'(D) + \frac{1}{1-r} \left(\frac{1}{r} \lambda'(D/r) - \lambda'(D) \right) = \frac{f'(\lambda(D)) - r^2 f'(\lambda(D/r))}{r(1-r)f'(\lambda(D))f'(\lambda(D/r))}.$$

Therefore, $\frac{\partial \gamma}{\partial D}(r, D) > 0$ if and only if $f'(\lambda(D/r)) < f'(\lambda(D))/r^2$, which proves the equivalence of conditions 1 and 2 of the Lemma.

Moreover, since $1/r > 1$ and λ is strictly increasing, then $\lambda(D/r) > \lambda(D)$. Thus, if f' is decreasing, we have $f'(\lambda(D/r)) \leq f'(\lambda(D)) < f'(\lambda(D))/r^2$, which proves condition 2 of the Lemma.

D.3. Proof of Lemma 5. As $0 < r < 1$ and λ is a strictly increasing function then, we have $D/r > D$ and $\lambda(D/r) > \lambda(D)$. Consequently, using the definition (B.2) of g_r , we have $g_r(D) > \lambda(D/r)$. According to the respective definitions (4.1) and (4.2) of the curves Φ_r and Γ_r , we deduce that the curve Φ_r is always above the curve Γ_r .

D.4. Proof of Lemma 6. The curves $\Phi_{1/2}$ and Γ are respectively defined by (4.3) and (4.4). Let us define the function $H : \left[0, \frac{m}{2}\right) \mapsto \mathbb{R}$ such that $H(D) = \lambda(2D) - g(D)$. According to Table 2, for a Monod function, the function H is defined explicitly by $H(D) = \frac{KmD^2}{(m-D)^2(m-2D)}$. Then, for any $D \in \left[0, \frac{m}{2}\right)$ one has $H(D) > 0$. Thus, for any $D \in \left[0, \frac{m}{2}\right)$, one has $\lambda(2D) > g(D)$ which means that Γ is always located strictly above $\Phi_{1/2}$.

D.5. Proof of Proposition 8. Let us prove that the Hill function satisfies Assumption 2. Straightforward computations show that

$$F(S) := \frac{f(S)f''(S)}{(f'(S))^2} = \frac{p-1-(p+1)(S/K)^p}{p}$$

Hence, for every $p \geq 1$, $F'(S) = -\frac{p+1}{K^p} S^{p-1} < 0$ and $F(0) = \frac{p-1}{p} < 1$, which proves that $F(S) < 1$ for all $S > 0$. Therefore, condition 4 of Lemma 3 is satisfied, which is a sufficient condition for Assumption 2 to hold.

Let us prove now that the Hill function satisfies Assumption 3. It is equivalent to prove that it satisfies the condition 2 of Lemma 4. Straightforward computations show that

$$\lambda(D) = \left(\frac{K^p D}{m-D} \right)^{\frac{1}{p}} \quad \text{and} \quad f'(\lambda(D)) = \frac{p}{m} \left(\frac{D^{p-1}}{K^p} \right)^{\frac{1}{p}} (m-D)^{\frac{p+1}{p}}$$

We have $0 < r < 1$ and $D < rm$ then, obviously, we have $0 < m - D/r < m - D$ and $0 < rm - D < m - D$. Thus, we obtain the following inequality

$$(m - D/r)(rm - D)^{\frac{1}{p}} < (m - D)(m - D)^{\frac{1}{p}}.$$

Straightforward calculations give

$$\frac{1}{r^2 m} (rm - D)^{\frac{p+1}{p}} < \frac{1}{rm} (m - D)^{\frac{p+1}{p}}.$$

Consequently, we have

$$\frac{p}{r^2 m} \left(\frac{D^{p-1}}{K^p} \right)^{\frac{1}{p}} (rm - D)^{\frac{p+1}{p}} < \frac{p}{rm} \left(\frac{D^{p-1}}{K^p} \right)^{\frac{1}{p}} (m - D)^{\frac{p+1}{p}}$$

which is equivalent to $f'(\lambda(D/r)) < f'(\lambda(D))/r$ and induces $f'(\lambda(D/r)) < f'(\lambda(D))/r^2$. This completes the proof of the Proposition.

D.6. Proof of Lemma 7. Let the function $H : \left[0, \frac{m}{2}\right) \mapsto \mathbb{R}$ be defined by $H(D) := \lambda(2D) - g(D)$. According to the analytical expressions of Table 2, we have

$$H(D) = K \sqrt{D} \left(\sqrt{\frac{2}{m-2D}} - \frac{3m-2D}{2(m-D)^{\frac{3}{2}}} \right).$$

Thus, $H(D) > 0$ gives $4mD^2 - 6m^2D + m^3 < 0$. The equation $4mD^2 - 6m^2D + m^3 = 0$ admits the two roots $D_1 = \frac{3-\sqrt{5}}{4}m$ and $D_2 = \frac{3+\sqrt{5}}{4}m$ such that $0 < D_1 < \frac{m}{2}$ and $\frac{m}{2} < D_2$. Therefore, for any $D \in \left(D_1, \frac{m}{2}\right)$ we have, $H(D) > 0$ which means that for any $D \in \left(D_1, \frac{m}{2}\right)$, the curve $\Phi_{1/2}$ is strictly below the curve Γ .

ACKNOWLEDGMENTS

The first author thanks the Algerian Government for her PhD grant. The authors thank the Euro-Mediterranean research network TREASURE (<http://www.inra.fr/treasure>) for support. The authors thank Jérôme Harmand for valuable and fruitful exchanges, and the anonymous reviewers for their constructive comments which have greatly improved this work.

REFERENCES

- [1] J. Monod, La technique de culture continue: theorie et applications, *Annales de l'Institut Pasteur*, **79** (1950), 39–410.
- [2] A. Novick and L. Szilard, Description of the chemostat, *Science*, American Association for the Advancement of Science, **112(2920)** (1950), 715–716.
- [3] D. Herbert, R. Elsworth and R.C. Telling, The Continuous Culture of Bacteria; a Theoretical and Experimental Study, *Microbiological Research Establishment*, Porton, Wiltshire, Great Britain, **3(14)** (1956), 601–622.
- [4] J. Harmand, C. Lobry, A. Rapaport and T. Sari, *The Chemostat: Mathematical Theory of Microorganism Cultures*, John Wiley & Sons, Chemical Engineering Series, 2017.
- [5] P.A. Hoskisson and G. Hobbs, Continuous culture—making a comeback?, *Microbiology—Sgm*, Microbiology Society, **151(10)** (2005), 3153–3159.
- [6] H.L. Smith and P. Waltman, *The theory of the chemostat: dynamics of microbial competition*, Cambridge University Press, Cambridge, **13**, 1995.
- [7] M. Wade, J. Harmand, B. Benyahia, T. Bouchez, S. Chaillou, B. Cloez, J. Godon, C. Lobry, B. Moussa Boudjemaa, A. Rapaport, T. Sari and R. Arditi, Perspectives in Mathematical Modelling for Microbial Ecology, *Ecological Modelling*, **321** (2016), 64–74.
- [8] L. Grady, G. Daigger, N. G. Love and DM. C. Filipe, *Biological wastewater treatment*, CRC press, (2011).
- [9] D. Dochain and P.A. Vanrolleghem, *Dynamic Modelling & Estimation in Wastewater Treatment Processes*, IWA publishing, (2001).
- [10] C.M. Kung and B. Baltzis, The growth of pure and simple microbial competitors in a moving and distributed medium, *Mathematical Biosciences*, **111** (1992), 295–313.
- [11] B. Tang, Mathematical investigations of growth of microorganisms in the gradostat, *Journal of Mathematical Biology*, **23** (1986), 319–339.
- [12] C. D. de Gooijer, W. A. M. Bakker Wilfried, H. H. Beeftink and J. Tramper, Bioreactors in series: An overview of design procedures and practical applications, *Enzyme and Microbial Technology*, *Biochemical engineering journal*, **18** (1996), 202–219.
- [13] G. Hill and C. Robinson, Minimum tank volumes for CFST bioreactors in series, *The Canadian Journal of Chemical Engineering*, Wiley Online Library, **67(5)** (1989), 818–824.
- [14] E. Scuras, A. Jobbager and L. Grady, Optimization of activated sludge reactor configuration:: kinetic considerations, *Water Research*, Elsevier, **35(18)** (2001), 4277–4284.
- [15] A. Rapaport, Some non-intuitive properties of simple extensions of the chemostat model, *Ecological complexity*, Elsevier, **34** (2018), 111–118.
- [16] I. Haidar, A. Rapaport and F. Gérard, Effects of spatial structure and diffusion on the performances of the chemostat, *Mathematical Biosciences and Engineering*, **8(4)** (2011), 953-971.

- [17] J. Harmand, *Contribution à l'analyse et au contrôle des systèmes biologiques application aux bio-procédés de dépollution*, Habilitation à diriger des recherches, Université C. Bernard Lyon, 2004.
- [18] J. Zambrano and B. Carlsson, Optimizing zone volumes in bioreactors described by Monod and Contois growth kinetics, Proceeding of the IWA World Water Congress & Exhibition, Lisbon, Portugal, (2014), 6.
- [19] J. Zambrano, B. Carlsson and S. Diehl, Optimal steady-state design of zone volumes of bioreactors with Monod growth kinetics, *Biochemical engineering journal*, Elsevier, **100** (2015), 59–66.
- [20] D. Herbert, Multi-stage continuous culture. Continuous cultivation of microorganisms, *Microbiological Research Establishment*, Porton, Wiltshire, Great Britain, 23–44 (1964).
- [21] I. Haidar, *Dynamiques Microbiennes Et Modélisation Des Cycles Biogéochimiques Terrestres*, Thèse de l'Université de Montpellier, 2011.
- [22] R. Fekih-Salem, C. Lobry and T. Sari, A density-dependent model of competition for one resource in the chemostat, *Mathematical Biosciences*, **286** (2017), 104–122.